

KWAME NKRUMAH UNIVERSITY OF SCIENCE AND
TECHNOLOGY, KUMASI
COLLEGE OF SCIENCE
DEPARTMENT OF MATHEMATICS



Numerical Simulation of Elliptic-Parabolic Problem for Two-Phase
Flow Model with Capillary Pressure

A THESIS SUBMITTED TO THE DEPARTMENT OF MATHEMATICS
THROUGH THE NATIONAL INSTITUTE FOR MATHEMATICAL SCIENCES
IN PARTIAL FULFILLMENT OF THE REQUIREMENTS FOR THE AWARD
OF
MASTER OF PHILOSOPHY DEGREE
(SCIENTIFIC COMPUTING & INDUSTRIAL MODELING)

By
Richard Owusu

MAY, 2017

DECLARATION

I hereby declare that, this thesis is the result of my own original research and that no part of it has been submitted to any institution or organization anywhere for the award of a degree. All inclusion for the work of others has been duly acknowledged.

<u>Richard, OWUSU</u>
Student (PG3325614)	Signature	Date

Certified By:

<u>Prof. I. K. DONTWI</u>
Member, Supervisory Committee	Signature	Date

<u>Dr. Peter AMOAKO-YIRENKYI</u>
Member, Supervisory Committee	Signature	Date

<u>Dr. Akoto Yaw OMARI-SASU</u>
Member, Supervisory Committee	Signature	Date

<u>Dr. R. K. AVUGLAH</u>
Head of Department	Signature	Date

Dedication

I dedicate this work to my loving and supportive parents, the late MR. and MRS. Emmanuel Atubiga Assibi and all my siblings. I appreciate you so much.

ABSTRACT

The study of multi-phase flow of fluids in reservoirs is of particular interest in the field of petroleum recovery. This process is studied with estimated or experimentally determined parameter values and some assumptions. Capillary pressure is one of the effective parameters influencing fluid flow in hydrocarbon reservoirs. However, it is assumed negligible by most researchers despite its importance. In this work, a two-phase (oil-water) flow with the effect of capillary pressure was modelled and transformed using fractional flow formulation. The model equations obtained from the fractional formulation comprise an elliptic-pressure equation and a parabolic-saturation equation. The Finite element (FE) method was employed to discretize the elliptic-pressure equation and the corresponding parabolic-saturation equation discretized by the Finite volume (FV) method. Results from the numerical simulation of the model revealed that capillary pressure has effect on saturation profile which was observed in diffusive dominated problems but with less effect in advective-diffusive problems which was observed at points where saturation gradient was high.

ACKNOWLEDGEMENTS

I wish to acknowledge and express my heartfelt gratitude to some groups of people who provided generous amounts of support and corporation during this study.

My sincere gratitude and appreciation to Dr. Peter Amoako-Yirenkyi, the supervisory committee, my lecturers, family, colleagues and friends for their outstanding support and guidance during this research. I am very grateful to all.

Finally, I will also want to show my appreciation to NIMS and all those who directly or indirectly contributed to this research.

Contents

DECLARATION	i
ABSTRACT	iii
ACKNOWLEDGEMENTS	iv
Declaration	v
Dedication	v
Acknowledgement	v
List of Tables	viii
List of Figures	x
1 INTRODUCTION	1
1.1 Background to the study	1
1.2 Statement of Problem	2
1.3 Objective	3
1.4 Outline of Methodology	4
1.5 Justification of Study	4
1.6 Organization of the Study	4
2 LITERATURE REVIEW	6
2.1 Reservoir Models and Formulation	6
2.2 Capillary Pressure for Two-Phase Models	10
2.3 Finite Volume and Finite Element Method	13

3	METHODOLOGY	18
3.1	Reservoir Rock and Fluid Properties	18
3.1.1	Porosity	18
3.1.2	Permeability (K)	19
3.1.3	Compressibility (C)	20
3.1.4	Density (ρ)	20
3.1.5	Viscosity (ϕ)	21
3.1.6	Fluid Velocity (\vec{v})	21
3.1.7	Wettability	22
3.1.8	Capillary Pressure	23
3.2	Partial Differential Equations	24
3.2.1	Classifications of PDEs	25
3.2.2	Linearity	25
3.2.3	Initial Conditions (IC) and Boundary Conditions (BC)	26
3.3	The Model	28
3.4	Mass Conservation	28
3.5	Conservation of Momentum (Darcy's Law)	31
3.6	The Two-Phase Flow Model	32
3.6.1	Saturation (S)	32
3.6.2	Capillary Pressure (P_c)	33
3.6.3	Relative Permeability ($K_{r\alpha}$)	33
3.7	Fractional Flow Formulation	34
3.7.1	Pressure Differential Equation	35
3.7.2	Saturation Equation	37
3.7.3	Fractional Flow Function	37
3.7.4	Residual Saturation	39
3.7.5	Relative Permeability Functions	40
3.7.6	Capillary Pressure Function	41
3.8	Model Assumptions	43
3.9	The Numerical Schemes	44

3.10	The Variational Method or Weak Formulation	45
3.11	The Finite Volume Method	48
3.12	The Finite Element Method	49
3.12.1	The Finite Element Basis Functions	50
3.12.2	One-Dimensional Elements	50
4	NUMERICAL IMPLEMENTATION OF THE TWO-PHASE FLOW MODEL	53
4.1	Problem Formulation	53
4.2	FE-FV Implementation for the Two-Phase Problem With Capillary Pressure Effect	55
4.2.1	Weak Formulation for the Pressure Equation	55
4.3	Well-posedness of the Problem	56
4.3.1	Lax-Milgram Lemma	57
4.3.2	Verification of the Conditions of Lax-Milgram Lemma	58
4.3.3	Finite Element Implementation for Pressure Equation	60
4.3.4	FVM for the Saturation Equation with Capillary Pressure Effect	61
4.3.5	Courant-Friedrichs-Lewy (CFL) Condition	63
4.3.6	Approach to Solving the Coupling Pressure-Saturation Equa- tion	64
5	NUMERICAL RESULTS, DISCUSSION AND CONCLUSION	65
5.1	Numerical Results and Discussion	65
5.2	Investigating the Effect of Capillary Pressure	68
5.2.1	Capillary Pressure Effect on Flow Rate	68
5.2.2	Capillary Pressure Effect on Saturation Profile	69
5.3	Conclusions	70
5.4	Recommendation	71
	References	76

List of Tables

3.1	Classification for Second-Order Linear PDE	25
3.2	Test functions $v_j(x)$ used in the method of weighted residuals and the method produced. Source: (George and Spencer, 1999)	47

List of Figures

3.1	Random packing of rocks of irregular shapes	18
3.2	Wettability and Contact Angle	22
3.3	Capillary pressure in an oil-water system. Source: Glover Paul . . .	23
3.4	Control Volume	29
3.5	The fractional flow curve as a function of Water Saturation	38
3.6	Brooks-Correy relative permeability curve for wetting and non-wetting phase	41
3.7	A capillary pressure-saturation curve during drainage (Brooks-Correy Capillary pressure function).	42
3.8	Drainage and imbibition capillary pressure functions. Source: L. P. Dakes (1978)	43
3.9	(a)Box basis function (b) Left and right half hat basis functions. . .	51
3.10	Basis functions for quadratic Lagrange interpolation.	52
3.11	Basis functions for degree d Lagrange interpolation at node i	52
5.1	Plot showing the Pressure profile, (p) along the distance for different time values	66
5.2	Pressure profile at $t=0$ (Blue), $t=0.25$ (Red), $t=0.5$ (Magenta), $t=1$ (Green)	66
5.3	Surface plot of Pressure profile (p)	67
5.4	Plot showing the saturation profile (S_w, S_o) of water and oil along the distance for different time values	67
5.5	(a) Capillary pressure function ; (b) water saturation distribution as a function of distance in the displacement path. (Source: L. P. Dakes, 1978)	68
5.6	Fluid flow by diffusion ($p_c \neq 0$)	69

5.7 Comparison of Saturation (S_w) profile for fluid flow by advection/diffusion with advection	70
--	----

Chapter 1

INTRODUCTION

1.1 Background to the study

Many phenomena in nature, such as heat conduction or convection, stress in mechanical structures, electromagnetic fields, and fluid mechanics are described by partial differential equations involving spatial derivatives of first and second order and time derivatives of multidimensional functions (Heckbert, 1993). Researchers from science and engineering started exploring and investigating fluid flow and transport in subsurface reservoirs and to use the information acquired to forecast, manage and control the physical processes as it takes place in a system. This kind of study often represent the reservoir, with all suitable physics, reservoir properties and geology as close as possible. According to Bastian (1999), a body which consist of a matrix (a solid part), with pore space filled with one or more fluids is referred to as a porous medium.

Mostly petroleum resources are discovered from rocks with enough interconnected void space which stores and transports fluids. Fluid flow in a reservoir takes place on a micrometer scale within the pore space of the porous medium. On the contrary, hydrocarbons are generally carried in rock zones which are some meters thick but extending a number of kilometers in the lateral directions (Knut-Andreas and Bradley, 2016). To observe the dynamic behavior of fluids and to measure the relevant subsurface reservoir parameters require much effort having a large degree of uncertainty attached in predicting its performance. As a result, simulation studies are normally performed to measure the level of uncertainty. In reservoir simulation, a numerical model of the petrophysical and the geological properties of petroleum reservoirs is used in analyzing and predicting the behavior of fluids in porous media

over some time. With reservoir modeling, multi-phase flow models embrace the properties of the reservoir domain together with motion of multiple fluids (ranging from immiscible/incompressible to miscible/compressible fluids) through the void space of a porous medium. In multi-phase flow, fluids flow together, allowing distinct interface between phases due to phase pressure differences (Nordbotten and Celia, 2012). According to Bear and Bachmat (1991), a chemically homogeneous part of a system being parted from other by a clearly defined physical boundary or interface is called a *phase*. In cases of single-phase systems, a single fluid (e. g. water) or a number of fluids totally mixed together with each other fills the pore space of the porous medium.

The partial differential equations for the two-phase fluid flow model in reservoir simulation describing flow of fluid in a porous medium are mostly non-linear and parabolic. In this study, the system of parabolic equations obtained for the two-phase model is reconstructed or remodeled into a system which consists of an elliptic pressure equation and a parabolic saturation equation by using the concept of fractional flow formulation. These equations are typically hard to solve analytically hence numerical schemes are employed. Some of these numerical schemes mostly used in reservoir simulation studies are the classical IMPES (Implicit-Pressure-Explicit-Saturation), the finite-volume method and the finite-element method. The numerical scheme considered in this study follows the approach of Luna and Hildago (2015), which solves the elliptic equation using the methods of finite-element and the parabolic equation through a finite-volume method.

1.2 Statement of Problem

The study of multi-phase flow models in reservoir modeling and simulation is of particular interest to researchers in the field of petroleum recovery. Of particular importance in reservoir modeling are the parameters used in developing the model which comes with a number of assumptions. Some of these parameters considered in

reservoir modeling are discussed in Section (3.1). In particular, the main objective of researchers in the field of reservoir simulation is to explore and investigate *fluid flow* and *transport* in subsurface reservoirs and to use this information acquired to forecast, manage and control the physical process of the system. According to Salarieh et al. (2016), capillary forces are one of the effective parameters in hydrocarbon reservoirs which are notable in porous media. It is one of the input parameters in reservoir modeling and simulation process which affects the flow and transport of fluid in reservoirs. Brooks and Correy (1964) theoretically established a relation between fluid saturation and the capillary pressure (p_c). It is observed that increasing saturation of wetting phase decreases the non-wetting phase saturation, hence, a reduction in p_c . According to literature, the greatest effect of capillary pressure on dynamic processes is observed in situations where there is large saturation gradient (e.g. at shock fronts) (Dake, 1978). Neglecting the effect of capillary pressure in such situations will in effect affect the performance of the model. Despite the importance of the capillary pressure, many researchers including Luna and Hildago (2015) assume it to be negligible, neglecting its effect in modeling and simulation, which may affect reservoir management and control of the physical processes of the system.

1.3 Objective

The study of Luna and Hildago (2015), on two-phase flow problem with the assumption of a zero capillary pressure gives this thesis the opportunity of extension with the following objectives. This study seeks to:

1. model the two-phase immiscible fluid flow model with the effect of capillary pressure forces.
2. solve the flow model (with and without the effect of capillary pressure) using the combined finite element-finite volume method.
3. investigate capillary pressure effect on the two-phase flow model.

1.4 Outline of Methodology

To achieve the objectives outlined in Section (1.3), the finite element-finite volume method is employed. As a result of two classes of partial differential equations cropping up from fractional formulation of the flow model, a combination of these two methods (finite element and finite volume method) is employed. The elliptic part of the problem is solved by the finite element method and the parabolic/hyperbolic part by the finite volume method. The data used for this study is a standard reservoir data.

1.5 Justification of Study

Capillary forces are one of the effective parameters in hydrocarbon reservoirs which are notable in the porous media (Salarieh et al., 2016). It is one of the input parameters in reservoir modeling and simulation process which affects fluid distribution in reservoir and fluid flow. Studying the effect of capillary pressure on saturation profiles is relevant in reservoir simulation as a result of its relation to the phase saturation and distribution of pore size of the porous media.

This study will explore the contribution or the capillary pressure effect on saturation profile. This in effect will help to predict reservoir performance under the action of capillary pressure.

1.6 Organization of the Study

This study is organized into five chapters.

- The first chapter gives an introduction to the study by presenting the background information, problem statement and the objectives of the study.
- Chapter two is the review of relevant literature.

- The third chapter is the outline of the methodology, in which the two-phase flow model is mathematically modeled to include the capillary pressure effect. In addition, the Finite element and the Finite volume methods as used in this study are reviewed in this chapter.
- Chapter four presents the numerical implementation of the two-phase flow model.
- In the fifth chapter, the numerical results obtained from the simulation are presented and discussed. Conclusions and some recommendations are as well outlined in this chapter.

Chapter 2

LITERATURE REVIEW

2.1 Reservoir Models and Formulation

According to Tore and Eyvind (2008), a number of ways in formulating equation system for two-phase flow modeling in a porous medium is explored. It is realized that the system of equations describing how the phases are accumulated, transported, and injected/produced in the model are coupled. This partial differential equations and the auxiliary conditions permits equation manipulation so that the dependent variables of interest are the main differences between the system formulations. In their work, five different formulations were tested for two-dimensions and one 1-dimensional formulation. Tore and Eyvind (2008) compared these formulations according to their numerical performances such as robustness (numerical stability) and the time taken to solve the problem. Six main types of equation system formulations were considered in this study which include; Partial pressure formulation, Buckley-Leverett formulation, Flooding formulation, Phase pressure-saturation formulation, Fractional flow formulation and the Weighted pressure formulation. The tests performed in their study revealed that the fractional flow formulation is the best and most robust formulation.

The main objective of the work done by Yufei et al. (2007), is the reconstruction of the two-phase model for fluid flow in a porous medium using fractional formulation approach and its applications. The IMPES (IMplicit-Pressure-Explicit-Saturation) concept is introduced for the fractional flow (FF) formulation using a finite volume element (FVE) method. It was stated that a more adaptive possibilities are proposed for the FF system depending on the differences that occurs between the fractional flow (FF) formulation and the fully coupled (FC) formulation. In order

to have a clear description and explanation to the differences between both formulations (fully coupled and fractional flow formulation method) and to have a clear perspective of the possible methods for fractional formulation, this work compared the adaptive techniques and numerical results obtained from the two formulations. The same numerical technique i.e., vertex-centered finite volume element method was used to discretize the fully coupled equation and the fractional flow equation with implicit scheme and IMPES respectively. Depending on the formulation and the technique to discretize the model an upwind scheme was employed for the two equations of the fully coupled formulation and for the fractional formulation the upwind scheme was employed only for the saturation equation. Numerical results and CPU times were presented and compared for both formulations and was realized that the fractional formulation was found efficient for advection-dominated two-phase flow problems. In addition, it was realized by Yufei et al. (2007) that the fractional flow formulation provides a considerable possibility for adaptive methods, and besides this, the fractional formulation makes it possible for a combination of different methods of discretization, one for pressure and another for saturation equation.

An introduction of existence of results and approximation technique for two-phase flow equations in a porous medium was done by Michael and Ben (2008). In order for the capillary pressure function to be generated for extreme saturations, it was assumed that the medium considered for this study could have hydrophobic and hydrophilic elements. The main objective of their study was the outflow boundary conditions modeling an open space interface. Since a maximum principle was not satisfied by any of the unknown pressure values p_1 and p_2 in their model considered, and also on the outflow boundary no condition was satisfied by the global pressure, the uniform boundedness for solution of the two-phase flow system becomes hard to prove. However in their work, Michael and Ben contributed to literature by deriving uniform bounds for solutions of two-phase system having outflow boundary conditions.

Aarnes et al. (2007) observed that fluid transport in petroleum reservoirs take place on a broad variety of physical scales posing great challenge to reservoir modeling and simulation since effects posed by fine-scale reservoirs mostly have a very great effect on flow patterns on large scales. Therefore to have a very reliable quantitative and qualitative results of simulation, it is very crucial to resolve all relevant scales and the interactions there in. In order to bring under control the challenge of multi-scale in modelling and simulation, it is a usual practice to use the technique of upscaling or homogenisation. In this procedure, one represents the reservoir characteristics or properties by some averaged properties, and solving the flow problem on coarse grids. A number of upscaling procedures give results that are reliable for only a small scope of flow scenarios which is unfortunate. As a result of the increased in demand for reservoir simulation studies, a more rigorous multiscale methods have been developed which absorb subscale effects more directly. In this work, some important scales for flow simulations were generally reviewed. Again, they presented and discussed a number of upscaling methods that have played a role in reservoir simulation history. Finally, they presented some more current procedures for scale modelling in the flow simulations hinged on the multi-scale paradigm. In conclusion, the advantages and the disadvantages of the use of multi-scale methods, instead of the traditional upscaling procedures in reservoir simulation were discussed. It was observed that solutions produced on both the fine scales and coarse scales by the multi-scale methods were accurate, and consequently it could be utilized as an efficient estimate fine scale solution techniques or a robust upscaling techniques. It becomes more flexible in choosing a solution technique to solve the saturation equation, since fine scale velocities are accessible at comparatively low cost of computation. The success of upscaling technique for saturation equations is very limited. Taking this into account will be helpful in performing the transport on a very fine grid affordable, and a fine scale velocity field may assist one to choose such a grid and also to ensure that the resulting solution is valid.

Several related formulations of the flow equations were reviewed by Lee and Froehlich (1986) which include the primitive shallow-water equations, which consist of an equation for conservation of momentum in each coordinate direction and an equation for conservation of mass. Appropriate boundary conditions for the problem were reviewed. The use of equal-order and mixed interpolation with various formulations of the flow equations were discussed. It was seen that both mixed interpolation and derivative or wave-continuity equation formulations are useful techniques for avoiding spurious oscillations. The treatment of specified velocities, discharges, stresses, and water-surface elevations as either essential or natural boundary conditions was discussed. It was seen that there are many possible ways of handling any given boundary condition. Finally, Galerkin's method of weighted residuals were also reviewed using several alternatives. Both point collocation and least squares methods offer the promise of being effective techniques for solving shallow-water equations.

The pressure at a grid-block containing a well differs from the average pressure in the same block and the bottomhole flowing pressure for the well (Chen and Zhang, 2009). To account for the difference, several finite difference models for wells are developed. The work done by Chen and Zhang (2009), discusses a systematic approach in deriving well models for other numerical techniques like the standard finite-element, control volume-finite element, and the mixed finite-element technique. In order to check the accuracy of the these well models, numerical results for an example of simple well demonstrating refinement effects of local grid were presented. The numerical results obtained from the study revealed less than 0.01 absolute error on the computation for pressure, showing the numerical model is accurate.

2.2 Capillary Pressure for Two-Phase Models

According to Brooks and Correy (1964), most of the literature describing fluid flow of two immiscible fluids makes simplifying assumptions that are in most cases far from realistic. They pointed out that in real cases, there exist functional relations among the saturation, the pressure difference between air and water (capillary pressure), and the permeabilities of air and water hence their study focused on describing these functional relations and the characteristics of the porous media affecting them. To achieve this objective, Brooks and Correy (1964) presented a theory following the Burdine approach which establishes the functional relations among saturation, difference in pressure, and air and liquid permeabilities in relation to hydraulic properties of the porous medium. The techniques employed to determine these hydraulic properties from the capillary pressure - desaturation curve were discussed. In addition, from the hydraulic properties which were determined experimentally, permeabilities of liquid and air as functions of saturation and capillary pressure were established. This theory presented by Brooks and Correy (1964) also reports on the necessary conditions for similarity between any two flow systems in a porous medium with two immiscible fluid phases occupying it. The non-wetting phase in this case is static while flow of wetting phase is by the law of Darcy. The experimental evidence presented indicates that these functional relations (for isotropic media) can be described in terms of two pertinent soil parameters, one of these parameters is called the "bubbling pressure" which is in relation to the maximum pore-size distribution and forms a continuous network or flow channels inside the medium. The other parameter is called the "pore-size distribution index" evaluating the distribution of sizes of the flow channels within a particular porous medium.

According to Shams et al. (2015), Engineers researching in the field of numerical reservoir simulation usually consider the use of capillary pressure to initialize the model. Nevertheless, capillary pressure effects on performance of petroleum reservoirs might not be understood fully for different flow processes. The principal

goal of this study was to present the oil-gas and water-oil capillary pressure effect on performance of petroleum reservoirs for reservoirs which produce under water injection, gas injection and natural depletion recovery processes on a number of reservoirs and production parameters. The naturally fractured and conventional reservoirs were investigated. With naturally fractured reservoirs, an investigation of both the fracture and matrix capillary pressures effect were done in the event where the driving force is only the capillary pressure imbibition and in the case when both capillary pressure imbibition and gravity drainage recovery processes are both active. The simulation results of small and large transition zones were compared to the results of models of zero transition zones. And three difference indicators were estimated for each run in order to quantify the effect of the capillary and the gravitational forces. These effects on different reservoir heterogeneity levels were quantified by performing hundreds of runs of the model. For different recovery processes, it was realized that effects of capillary pressure were different. Though the capillary pressure is found to be important for model initialization, it may be of less importance during flow calculations in all situation, they reported. In depletion runs capillary pressure was found to be more important than in most displacement runs. Studying on the relation between reservoir heterogeneity level and the effects of capillary pressure, no clear correlation was found to exists between them. Under certain conditions for naturally fractured reservoirs, it was again realized that effects of the fractured gas-oil capillary pressure increase. To validate the conclusions drawn from this study, Shams et al. (2015) used a reservoir model to affirm the results obtained from the hypothetical models.

Botero et al. (2016), studied the effect of Dynamic capillary pressure in Two-Phase flow in a porous medium. There exist theories which propose the capillary pressure dependence on both saturation and time rate of change of saturation. From this study, the significance of dynamic effects on the relationship between capillary pressure and saturation was investigated through experiments in a homogeneous porous medium. A number of laboratory experiments were conducted involving

motion of two immiscible fluids, water and Tetrachloroethylene (PCE), in a homogeneous column. The experiments consisted of a continuous cycle of imbibition, and drainage, where a large pressure of 20kPa is applied to the displacing fluid. Contrary to traditional procedure, no hydrophobic or hydrophilic membranes were used in this experimental set-up. In this paper, the experimental set-up was described and preliminary results were presented as well.

Two-phase flow in a porous medium with heterogeneous capillary pressure functions was examined in the work done by Helmer and Steinar (2011). In literature, a very little attention is been drawn to this problem which creates challenges for numerical discretization. This results from saturation discontinuities arising from the interface of regions with different homogeneities in the domain. A standard scheme possessing an important characteristic (at the discrete level) of being pressure continuous was employed for the discretization with harmonic mean of the absolute permeability as the basis for the scheme. Nevertheless, a recent multi point flux approximation scheme, was extended to count for two-phase flow so as to look into 2-D flow phenomena by an accurate numerical method. At discrete level, the multi point flux approximation scheme was found to be pressure continuous and was employed in discretizing two-phase flow pressure equation in fractional formulation which is appropriate for capillary heterogeneity. Helmer and Steinar (2011) after investigating one-dimensional flow problem with known semi-analytic solution, found out that the best numerical results was given by the usage of standard schemes hinged on harmonic mean of the absolute permeability. The flow problem was solved in an implicit-pressure explicit-saturation setting, employing fractional formulation approach, appropriate for capillary pressure heterogeneity. By the use of second-order central upwind scheme, the other part of the equation, the saturation equation, for the two-phase flow model was discretized. By employing both unstructured triangular grids and structured quadrilateral, some numerical examples were presented to demonstrate the relevance of capillary pressure heterogeneity in two-dimensional two-phase flow. In the study, a significant effect of the

capillary pressure heterogeneity was observed on the water breakthrough. Hence it would be practicable presuming the effect of capillary heterogeneities in complex real reservoirs to be significant.

2.3 Finite Volume and Finite Element Method

Generally on a given grid, there is an extensive study on the means to develop numerical schemes for problems of partial differential equations. One of these schemes applied to structured grid is the classical finite difference scheme. Shashkov (1996) proposed mimetic finite difference scheme which is more favourable when working on highly unstructured grids. The analysis on the convergence as well as the super convergence for this proposed scheme by Shashkov (1996) for smooth problem on a smooth mesh was also studied by reconstructing the scheme in a mixed finite-element method form (Berndt et al., 2005). However the cost of computation for these schemes was a concern. The finite difference scheme poses a number of restrictions which is solved by the Finite volume methods which are normally locally mass conservative. Studies shows that, the theory of finite-volume for diffusion equation which comes with scalar coefficient on unstructured mesh has advanced significantly. Some of these applications can be found in the work of Lazarov and Mishev (1996) and Mishev and Qian-Yong (2016). With the assumption of smooth meshes, the convergence for one of these schemes, the multi-point flux approximation, on quadrilateral grids is proven (Klausen and Winther., 2014). Consider the domain Ω . Eymard et al. (2016) built an approximate gradient of an elliptic problem solution in Ω which was later proven to be convergent in $H_{div}(\Omega)$ by the use of classical finite-volume piecewise constant approximation of the solution. They stated that when the solution is in $H^2(\Omega)$ an error estimate is given. The control volume finite-element method, mostly called finite volume element method is one other possibility worthy of consideration in the finite volume approach which Huang and Xi. (1998) studied for general self-adjoint elliptic problems. These methods are mostly locally mass conservative and are applied on grids which are flexible,

however they fail in preserving the differential operator symmetry, and never yield direct estimation of the velocity field.

The ideas of finite element analysis date back much further. It was first introduced by Courant (1943). The technique whereby an approximating function which is required in a piecewise application for any method of variation is referred as the finite-element method. The work of Courant (1943) introduces the use of piecewise continuous functions in the applied mathematics literature. These functions are defined on triangular domains. The idea of minimizing a functional by the use of linear approximations over sub-domains was developed by Courant. The values of these approximating functions are only specified at the discrete points of the sub-domains referred to as nodes of a mesh of elements. In 1942, Richard Courant published his paper to the American Mathematical Institute adding a two-paged example on how the methods of variation introduced by Lord Rayleigh in 1877 can be widely used in potential theory. In this example, he employed piecewise-linear approximations on a set of triangles referred by him as "elements," to solve some examples on two-dimensions - and the Finite-element was born (Pelosi, 2007). Engineers and mathematicians, from 1950s to 1970s developed the finite element method into a general method to solve partial differential equations numerically.

Lee and Froehlich (1986) in his work reviewed publications on the the finite-element methods applied to solving two-dimensional surface-water flow equations in horizontal plane. According to Lee and Froehlich (1986), finite-element methods are more convenient to model two-dimensional flows on complex geometry with spatially variable resistance. A two-dimensional finite-element surface-water flow model with depth and vertically averaged velocity components as dependent variables gives the user a higher level of flexibility in defining the geometric properties of the medium like the boundaries of a channel, islands, water bodies, embankments and dikes.

In solving the one-dimensional convection-diffusion equation with a trapezoidal-

rule scheme, Price et al. (1968) showed that finite-element method takes lesser nodes and lesser time for computation than the finite-difference method to achieve comparable accuracy. Furthermore, to solve equations of one-dimensional gravity-wave motion where both depth and grid are variables of interest, Thacker (1978) also showed that finite-element solutions were more accurate in comparison to solutions of finite-difference. Johnson et al. (1984) studied on finite-element method for linear hyperbolic problems which gave a survey of some recent work on finite-element method for convection-diffusion problems as well as first-order linear hyperbolic problems.

Comparing the two methods, the works of Idelsohn and Onate (1993), and Zienkiewicz and Onate (1990) compared the finite-element and the finite-volume methods, showing that the Finite Volume method shares the theoretical basis of the finite-element method, since it is a particular case of the Weighted Residuals Formulation. However, the weighting used in the first (constant volumes in the case of first order approximation) allows to take advantage of some properties of conservation, and the resolution algorithms are posed in a very advantageous way.

The most common mathematical models that represent two-phase problems are represented by a system of parabolic equations with the variables of interest being pressure and saturation of the different phases involved in the process. In literature, these parabolic problems are remodelled into a system consisting of an elliptic and a hyperbolic equation for pressure and the saturation respectively (Yufei et al., 2007). As a result of these two different kinds of partial differential equations, different numerical schemes are carefully chosen in literature for each particular partial differential equation some of which combines two different methods for the problem.

In solving numerically system of partial differential equations that arise from Black-Oil model, Bergamaschi et al. (1998) proposed a sequential coupling of mixed-finite

element and shock-capturing finite-volume techniques. The Brezzi-Douglas-Marini space of degree one (BDM1) was employed in approximating Darcy's velocity in the pressure equation which is parabolic in nature, while a higher order Godunov type scheme, which in this study was extended to triangle based unstructured grids, was used in solving the system of mass conservation laws. In this work, a sequential coupled mixed finite-element/shock-capturing finite volume method was developed and it was applied to the numerical approximation of the solution of time-dependent two-dimensional equations of the Black-Oil model. It was stated in their work that in treating the phase pressure and the velocity simultaneously, the high-order mixed finite-element is one of the numerical schemes that accurately solves the problem. On the contrary, shock-capturing finite-volume method exhibits the characteristics of resolving accurately steep gradient without spurious numerical oscillations while taking numerical dissipation effects at very low levels. In this case one usually considers conservative formulation, which allows one to accurately predict the moving discontinuities that appears in the physical solution. The numerical results obtained on 1-D and 2-D test cases prove the effectiveness and the robustness of the coupled mixed finite-element and shock-capturing finite volume techniques. The coupling concept seems particularly suitable to handle high heterogeneities and simultaneously fixing accurately steep gradients without spurious oscillations.

Luna and Hildago (2015) used a combined finite element and finite volume technique for simulating the solution to the two-phase flow model obtained in their work. Fractional flow formulation for two-phase flow model was used in the work of Luna and Hildago (2015). In their study, they obtained the solution of the model numerically by using both the techniques of finite-element and the finite-volume. The values of the cell interface velocities of the finite volume mesh was obtained from point-wise pressure values at the finite element nodes with second-order non-oscillatory reconstruction procedure. According to Luna and Hildago (2015), the choice of these two different methods for the same problem was because finite-element methods were specifically designed to be used for elliptic (and parabolic) problems. However

applying it to hyperbolic problems, finite-element fail in its standard or traditional formulation, essentially when there is discontinuity of solutions. On the other hand, finite-volume methods do well in these cases since discontinuous solutions are well propagated by finite-volume methods. The numerical results obtained for their study were compared to the results of ECLIPSE (commercial code) which shows appropriate behavior from qualitative point of view. The treatment of two-phase flow problem was proven effective and appropriate in terms of the saturation solution in comparison to the results from ECLIPSE. The advance of the saturation front in this problem was controlled by the fractional flow rate derivatives to water saturation.

Chapter 3

METHODOLOGY

3.1 Reservoir Rock and Fluid Properties

The amount of petroleum reserves in a trap and the rate at which this can be recovered depends basically on the characteristics of the trapped rock and the kind of fluids it is contained in the rock. Certain characteristics are determining factors of the total amount of petroleum in place; other properties also limit the fraction of this amount in place that can be reproduced. In addition, the flow rate of fluids in a reservoir is determined basically by some other rock properties and in addition with some other fluid properties.

3.1.1 Porosity

In conventional petroleum reservoirs, hydrocarbons, like crude oil or natural gas, are basically trapped in place by overlying rock formations which has a very low permeability. They are found in pore spaces between the grains of porous sedimentary rocks. These rock grains are irregular in shape, resulting in many pores left between the rock grains (Figure 3.1).

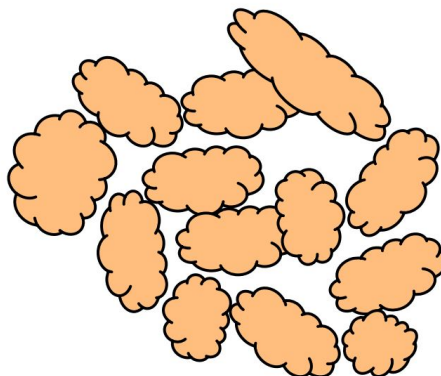


Figure 3.1: Random packing of rocks of irregular shapes

The spaces between the rock grains are termed as *pores* and the total amount/volume of pore space in a sample of a particular rock is known as its *pore volume*. The net volume of grains is termed *grain volume*. The total volume of a rock sample termed the *bulk volume*, V_b which is the sum of both the grain volume, V_g , and the pore volume, V_p . Another primary rock property called the *porosity*, ϕ , which is the fraction of pore volume to the total volume of a rock sample. Mathematically:

$$\phi = \frac{V_p}{V_b} \quad (3.1)$$

In a reservoir, pore spaces between rock grains can be interconnected that contributes to fluid flow or permeability. The interconnected pore spaces in a rock contributing to fluid flow or permeability in reservoirs is called the *effective porosity*, ϕ_e . *Residual porosity*, ϕ_r , is the isolated and non-connected pore spaces which trap fluids in place and hence do not contribute to fluid flow. *Total porosity* is the total volume of pore space in the rock grain that contributes to fluid flow or not. Mathematically;

$$\phi_t = \phi_r + \phi_e \quad (3.2)$$

3.1.2 Permeability (K)

This property is the rock's ability to conduct or transmit fluids through its interconnected pores. Different fluids experience different permeabilities in the same sample of rock. Increasing permeability leads to increasing fluid flow through the medium under a given set of conditions. The earliest attempt at measuring permeability was in 1856 studied by Henry Darcy. Permeability is termed *specific/absolute permeability* in a porous medium where the medium is completely saturated with one phase. However in cases of multi-phase flow, relative permeability is considered.

The ratio of of a fluid's effective permeability at given saturation to the absolute permeability of the medium at total saturation is referred as *Relative permeability*. The measure of conductance of a porous medium for one fluid phase when more

than one fluid saturate the medium with is called the *effective permeability*.

3.1.3 Compressibility (C)

For a unit change in pressure under certain conditions, the volume of a particular substance changes. This property of a substance is called *Compressibility*. Let C , V and P be compressibility of a substance, volume of substance and pressure respectively, then compressibility is defined mathematically as:

$$C = -\frac{1}{V} \left(\frac{\partial V}{\partial P} \right). \quad (3.3)$$

The negative sign in equation (3.3) is added to give a positive compressibility. This is due to the fact that the volume of a particular substance always decreases with increase in pressure hence the partial derivative in (3.3) will be negative. Therefore, the minus sign is added to give a positive compressibility value. At constant temperature, equation (3.3) describes the change in volume of substance during a change in pressure. When the pressure of the internal fluid inside the void spaces of a rock grain, subjected to a constant external pressure, is reduced, the rock's bulk volume decreases with increase in the volume of the solid rock materials (Craft and Hawkins, 1991). This volume change slightly reduces the porosity of the rock, indicating that rock porosity depends on pressure due to rock compressibility. If pressure falls due to production or extraction of fluid, there is compression of rocks hence reduction in porosity. Fluids can be considered as incompressible, slightly compressible and compressible. Gases are highly compressible compared to oil and water which are mostly considered incompressible in flow modeling.

3.1.4 Density (ρ)

The density of a solid or a fluid generally depends on the temperature and pressure of the fluid. However in isothermal system, temperature is considered constant. The compressibility (the pressure dependence of density) of a solid matrix and water can be considered negligible. However because of the high compressibility of

gas, pressure effect on density must be considered in reservoir studies.

3.1.5 Viscosity (ϕ)

Viscosity is another important fluid property which measures the resistance of a fluid to flow. Fluids obey Newton's Law of Viscosity (equation 3.4). To be specific, viscosity determines the temporal angle deformation τ of a fluid caused by a given applied shear stress τ ,

$$\tau = \mu \frac{\partial \tau}{\partial t} \quad (3.4)$$

where, μ is the fluid's *dynamic viscosity*, and the kind of fluids following equation (3.4) are known as Newtonian fluids. In general, the dependence of viscosity on pressure is very low hence usually neglected. However, temperature T , has a strong effect, where μ decreases with T for liquids and increases for gases (Yufei et al., 2007). Viscosity of a fluid can be accounted for by Reynolds number (Re) expressed as:

$$Re = \frac{velocity \times distance}{Viscosity} \quad (3.5)$$

Low Re means flow of fluid does not change with time and high Re means flow of fluid changes with time.

3.1.6 Fluid Velocity (\vec{v})

In continuum mechanics, flow velocity in fluid dynamics is a vector field which is mathematically used in describing the motion of a continuum. Equation (3.6) which is the flow velocity

$$\vec{u} = \vec{u}(\mathbf{x}, t) \quad (3.6)$$

gives the velocity of a fluid element at position \mathbf{x} and time t . The length of the flow velocity vector is the flow speed and is a scalar. Fluid velocity effectively describes the motion of fluids and many other physical properties of fluids can as well be written mathematically in terms of the flow velocity.

3.1.7 Wettability

Fluids have a preferential attraction to itself, and the relative strength of the cohesive forces result in surface tension which develops on a fluid-fluid interface. However, molecules of fluids may as well have a preferential attraction to solid interfaces. Suppose two fluids occupy a solid surface, the molecules of the fluid displaying the greatest attraction for atoms of the solid will be the fluid occupying the greatest part of the solid surface and consequently will displace the other fluid. In reservoir engineering, there is a likelihood for a fluid to spread over the surface of a solid in the presence of other fluids that are immiscible. The fluids interaction with the solid phases is referred as *Wettability*. It is the angle of contact, θ , between liquid droplets in thermal equilibrium on a horizontal surface. In a typical reservoir, the



Figure 3.2: Wettability and Contact Angle

magnitude of the adhesive forces decreases rapidly with distance to the wall (Bastian, 1999). The interaction with the cohesive forces leads to a specific angle of contact θ between the solid surface and the fluid-fluid interface that depends on the properties of the fluids. The fluid for which $0 < \theta < 90^\circ$ is called the *wetting phase fluid*, the other fluid is referred as the *non-wetting phase fluid*. In the first case of Figure 3.2, the wetting phase is water and in the second case, oil is the wetting phase. In the case of three immiscible fluids, each fluid is either wetting or non-wetting with respect to the other fluids. Real rocks may be completely water-wet, and indeed are commonly so. They may, however be oil-wet or neutrally wet or have a mixed wettability (depending on the contact angle, θ).

3.1.8 Capillary Pressure

The *capillary pressure* is the difference between the pressures in each of the two fluids forming an interface. The capillary pressure is proportional to the surface tension. Note that the greater of the two pressures is developed in the fluid which contains the center of curvature of the curved fluid interface. The pressure is proportional to the surface tension, but inversely proportional to the radius of the tube (Paul, 2016). As the radius of the tube increases, the capillary pressure decreases. The difference in pressure (the capillary pressure) causes the interface to rise up the capillary tube until the weight of the suspended column of fluid balances the capillary force that is associated with the capillary pressure.

In an oil-water system, consider Figure 3.3, the free water level is the height of the interface when the radius of the capillary tube tends to infinity (i.e., the capillary pressure is zero and $h=0$) as before. This interface exists at a given absolute pressure P_{FWL} . Capillary forces exist inside the restricted capillary tubing that result in the rise of the water to a height h above the free water level.

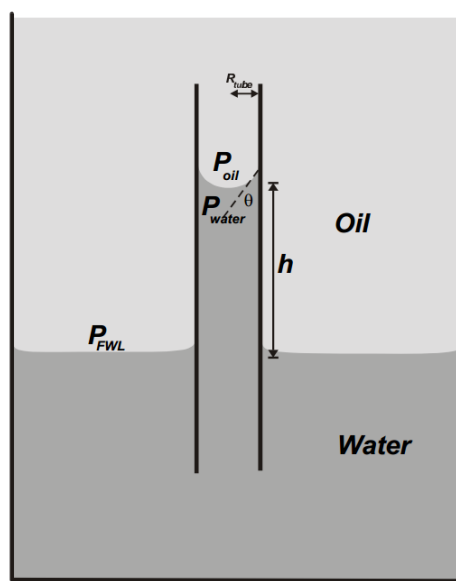


Figure 3.3: Capillary pressure in an oil-water system. Source: Glover Paul

In reservoirs, capillary pressure is an important parameter that needs to be considered due to its implications. Real rocks contain an array of pores of different sizes connected together by pore throats of differing size. Each pore or pore throat size can be considered heuristically to be a portion of a capillary tube.

3.2 Partial Differential Equations

Fluid dynamics in oil petroleum reservoir is governed by non-linear and complex systems of partial differential equations. In differential equations, one typically studies a few classes of problems for which there are closed form solutions, such as ordinary linear differential equations with constant coefficients. Most problems of interest in real world simulation are much more complex. They mostly involve domains of two or more dimensions or they come with nonlinear effects, yielding partial differential equations or non-linear differential equations respectively.

Partial differential equations states the relationship between a function of more than one independent variable and the partial derivatives of the function with respect to the independent variables. This is different from an *ordinary differential equation*, which comes with functions of only one variable. In most engineering and science problems, either space (x, y, z) or space and time (x, y, z, t) represents the independent variables. The dependent variable is dependent on the physical problem to model. If a function of two variables is denoted $p(x, y)$, then one may consider the following as examples of partial differential equations:

$$\frac{\partial^2 p}{\partial x^2} + \frac{\partial^2 p}{\partial y^2} = 0 \quad \text{Laplace's Equation} \quad (3.7)$$

$$\frac{\partial^2 p}{\partial x^2} - \frac{\partial^2 p}{\partial y^2} = 0 \quad \text{Wave Equation} \quad (3.8)$$

$$\frac{\partial^2 p}{\partial x^2} - \frac{\partial p}{\partial t} = 0 \quad \text{Heat Equation} \quad (3.9)$$

$$\frac{\partial^2 p}{\partial x^2} + \frac{\partial^2 p}{\partial y^2} = g(x, y) \quad \text{Poison Equation} \quad (3.10)$$

3.2.1 Classifications of PDEs

Generally, second-order partial differential equations in two independent variables x, y and the dependent variable $p(x, y)$ is of the form:

$$M \frac{\partial^2 p}{\partial x^2} + N \frac{\partial^2 p}{\partial x \partial y} + Q \frac{\partial^2 p}{\partial y^2} + R \frac{\partial p}{\partial x} + S \frac{\partial p}{\partial y} + Tp + Z = 0 \quad (3.11)$$

where M, N, Q, R, S, T, Z may be functions of x, y or constants in which case we have linear equation. If the term $Z \neq 0$, the PDE (3.11) is called Homogeneous and Non-homogeneous otherwise. The classification of (3.11) is dependent on the sign of the discriminant, $N^2 - 4MQ$, as follows:

Table 3.1: Classification for Second-Order Linear PDE

Discriminant	Classification of PDE
$N^2 - 4MQ < 0$	Elliptic
$N^2 - 4MQ = 0$	Parabolic
$N^2 - 4MQ > 0$	Hyperbolic

3.2.2 Linearity

A partial differential equation is *linear* provided the power of the dependent variable and its derivatives is one (1) (no product of the unknown function and its derivatives) and *non-linear* if otherwise. For example

$$\frac{\partial u}{\partial t} + t \frac{\partial u}{\partial x} = 0 \quad (3.12a)$$

$$\frac{\partial^2 u}{\partial x^2} + \frac{\partial^2 u}{\partial x^2} = 0 \quad (3.12b)$$

$$u_t - ku_{xx} = 0 \quad (3.12c)$$

$$u_t + uu_{xx} = 0 \quad (3.12d)$$

$$u_t \cos u - uu_{xx} = 0 \quad (3.12e)$$

Equations (3.12a,b,c) are linear while equation (3.12d,e) are non-linear. This is most easily described in the context of a differential operator \mathbf{L} , applied to a function u (defined $\mathbf{L}u = \frac{\partial u}{\partial x}$). The operator is said to be linear if for any two functions u, v and any constant c the following hold.

1. $\mathbf{L}(u + v) = \mathbf{L}u + \mathbf{L}v$ and
2. $\mathbf{L}(cu) = c\mathbf{L}u$

3.2.3 Initial Conditions (IC) and Boundary Conditions (BC)

Solutions to differential equations are infinitely many. The general solution to a differential equation of order n is indeed dependent on n arbitrary functions. For partial differential equations, the solution is singled out by specifying auxiliary conditions to the partial differential equation. Boundary conditions imposed on the boundary of the domain of interest are added to partial differential equations that models equilibrium processes. The solutions for partial differential equations that models dynamical processes are specified by imposing one or more conditions. The number of IC imposed on the equation is dependent on the highest-order time derivative appearing in the equation. In favorable circumstances, the initial and/or boundary conditions imposed on the equation helps in finding unique solutions. The addition of suitable boundary conditions to a partial differential equation is referred as *boundary value problem* whereas the partial differential equation together with boundary and initial conditions is referred as *initial-boundary value problem*.

There are three basic types of boundary value problems arising in a number of applications. Consider a linear partial differential equation of the second order

$$\mathbf{L}u = G(x, t) \tag{3.13}$$

where \mathbf{L} is a second order linear differential operator. Related to differential equation (3.13) we define the following boundary conditions:

1. *Dirichlet Boundary Condition:* Dirichlet BC usually corresponds to setting the value of a field variable on the boundary, i.e., the solution value is specified on the boundary. We usually write these conditions in the form

$$u(x, t)|_{\partial\Omega} = f(x, t) \quad (3.14)$$

2. *Neumann Boundary Condition:* Neumann BC usually specifies a flux condition on the boundary i.e., the normal derivative $\partial_n u(x, t)$ of the solution is specified on the boundary $\partial\Omega$, named after Carl Gottfried Neumann. This is written symbolically as

$$\partial_n u(x, t)|_{\partial\Omega} = g(x, t) \quad (3.15)$$

3. *Robin Boundary Condition:* We have Robin boundary condition if one specifies a linear combination of the solution and its normal derivative on the boundary. For some nonzero constants or functions a and b and a given function h defined on $\partial\Omega$, this condition can be expressed as

$$a u(x, t)|_{\partial\Omega} + b \partial_n u(x, t)|_{\partial\Omega} = h(x, t) \quad (3.16)$$

If $f(x, t)$, $g(x, t)$ and $h(x, t)$ in (3.14), (3.15) and (3.16) respectively, are identically zero in the domain, then we have *homogeneous boundary conditions*; otherwise, the boundary conditions are *non-homogeneous*. The kind of boundary condition can vary from point to point on the boundary, but at any given point only one BC can be specified.

In reservoir simulation, the boundary condition is such that the reservoir is assumed to lie within some closed curve C allowing no flow across its boundaries. Also fluid injection and production occurs at wells mostly referred as point sources and sinks. At the points where flow is not allowed, the boundary condition requires that the normal component of the vector \vec{v} at the curve C be set to zero which is comparatively a tough thing to do numerically for an arbitrary curve C . However,

since our domain of interest is mostly assumed to lie inside the interior of the reservoir, it becomes more adequate to represent the boundary of the curve in a way such that the reservoir is embedded in a rectangle (or rectangular parallelepiped). In reservoir modeling, the value of the normal component of the quantity is mostly specified representing flow across that boundary. However, one alternative means is to set a no flow boundary condition and placing fictitious wells at grid points on or near the boundary. Injection at such wells implies flow is into the region over the boundary, while production implies flow is out of the region across the boundary. Finally, it is also desirable to specify the value of the pressure at the boundary, rather than rate, in addition to the other possible boundary conditions.

3.3 The Model

The use of mathematical models of petroleum reservoirs started since 1800s. A mathematical model is made of a number of equations describing fluid flow in a conventional or unconventional reservoir, which comes with appropriate set of boundary and/or initial conditions (Zhangxin et al., 2006). The flow of fluids in conventional or unconventional reservoirs is governed by some basic principles which includes mass conservation principle, the conservation of momentum and energy and equation of states principle.

3.4 Mass Conservation

For a closed system, the conservation of mass principle is implicitly used by requiring that the mass of the system remain constant during a process. For control volumes, mass can be allowed to cross the boundaries and so the amount of mass entering and leaving the control volume Ω must be accounted for.

Consider an arbitrary volume Ω (Figure 3.4), fixed in space with a closed surface S bounding the space. The mass conservation equation states the balance between

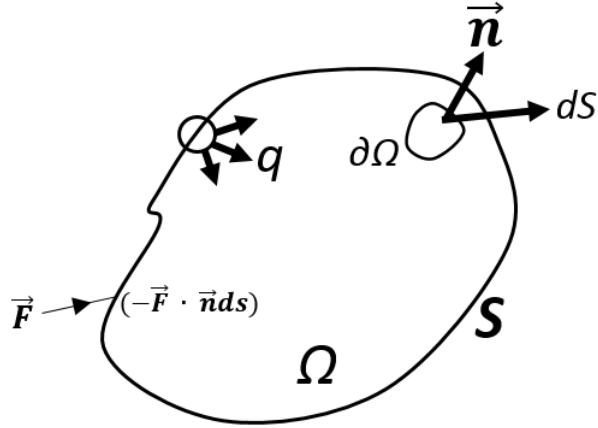


Figure 3.4: Control Volume

the rate of mass change in the arbitrary volume Ω , and inflow of mass through the boundary surface S . For a differential volume $\partial\Omega$, the mass of a fluid within Ω is defined as:

$$dm = \phi \rho d\Omega \quad (3.17)$$

which gives the total mass of the fluid in Ω as:

$$m = \int_{\Omega} \phi \rho d\Omega \quad (3.18)$$

where m , ϕ and ρ are respectively the mass of fluid, porosity and the fluid density. The time rate of change of mass m , in an arbitrary volume is expressed as

$$\frac{\partial}{\partial t} m = \frac{\partial}{\partial t} \int_{\Omega} \phi \rho d\Omega \quad (3.19)$$

In addition, the mass of the fluid varies through the effect of fluxes which expresses the contributions from the surrounding points and through the sources q . The net contribution from the incoming fluxes through the surface S , with a unit vector \vec{n} (pointing outward) for the surface normal is given as

$$- \oint_S (\vec{F} \cdot \vec{n}) ds; \quad \vec{F} = \rho \vec{v} \quad (3.20)$$

The flux represents the quantity which passes through the surface at a particular time or the flow rate of a property per unit area (surface). Finally the total contributions from the sources q , in the arbitrary volume, is given as

$$\int_{\Omega} q d\Omega$$

A general form for the law of conservation is expressed in stating that the rate of change of the mass of the fluid in an arbitrary volume Ω , must be equal to the sum of the contributions from the sources q and the net contributions from the incoming fluxes through S , with a unit vector $\vec{\mathbf{n}}$ (pointing outward) for the surface normal (Hirsch, 1988). Mathematically, the mass conservation equation is expressed in integral form as:

$$\frac{\partial}{\partial t} \int_{\Omega} \phi \rho d\Omega = - \oint_S (\vec{F} \cdot \vec{\mathbf{n}}) ds + \int_{\Omega} q d\Omega \quad (3.21)$$

From the divergence theorem

$$\oint_S (\vec{F} \cdot \vec{\mathbf{n}}) ds = \int_{\Omega} \nabla \cdot \vec{F} d\Omega, \quad (3.22)$$

the mass conservation equation (3.21) becomes

$$\frac{\partial}{\partial t} \int_{\Omega} \phi \rho d\Omega = - \int_{\Omega} \nabla \cdot \vec{F} d\Omega + \int_{\Omega} q d\Omega \quad (3.23)$$

Hence in the differential form, equation (3.23) is written as:

$$\frac{\partial}{\partial t} \phi \rho = -\nabla \cdot \vec{F} + q \quad (3.24)$$

By introducing the flux $\vec{F} = \rho \vec{v}$, the equation of mass conservation for a single phase is expressed as:

$$\frac{\partial}{\partial t} \phi \rho + \nabla \cdot \rho \vec{v} = q \quad (3.25)$$

In petroleum and natural gas calculations, volumetric factors were introduced by

researchers in order to be able to relate fluids volume obtained at the surface (stock tank) to the volume that fluids actually occupied when compressed in reservoirs. Mathematically

$$B = \frac{\text{Volume of phase at reservoir condition}}{\text{Volume of phase at standard condition}} \quad (3.26)$$

By introducing the volumetric factor $B = \frac{V}{V_s} = \frac{\rho}{\rho_s}$, equation (3.27) is obtained.

$$\frac{\partial}{\partial t} \left(\frac{\phi}{B} \right) + \nabla \cdot \frac{1}{B} \vec{v} = q \quad (3.27)$$

3.5 Conservation of Momentum (Darcy's Law)

Generally, the flow of fluid through a porous medium is modeled by Darcy's law, which is an expression of momentum. A fundamental law linking pressure drop and velocity in fluid flow through porous media is the law of Darcy (Wojciech and Anna, 2014). Darcy (1856) conducted an experiment on the flow of liquids through beds of sand and observed that the volumetric flow rate Q is directly related to the pressure difference between the inlet and the outlet of the medium, cross sectional area and inversely related to the length of the medium. Mathematically Darcy's law states:

$$Q = c \frac{A}{L} \Delta P \quad (3.28)$$

where the constant of proportionality c is related to $\frac{1}{\mu}$, (μ is viscosity). Hence we have the Darcy's equation with the absolute permeability K expressed as

$$Q = \frac{KA \Delta P}{\mu L} \quad (3.29)$$

Dividing through equation (3.29) by A , equation (3.30) is obtained as:

$$\vec{v} = -\frac{K}{\mu} \nabla P \quad (3.30)$$

where \vec{v} is called the Darcy's velocity. Equation (3.30) represents the case where flow is horizontal. However in the case where flow is both vertical and horizontal, we consider pressure change both in the horizontal direction and in depth. This results in the extended Darcy equation:

$$\vec{v} = -\frac{K}{\mu} \nabla(P + \rho gh) \quad (3.31)$$

where ρ , g and h are respectively density, gravity and height.

3.6 The Two-Phase Flow Model

The two-phase flow model considered in this study assumes no transfer of mass between the two fluids modeled. If the fluids are immiscible and separated by a sharp interface, they are referred to as phases. In two phase system, one of the fluids to be modeled wets the porous medium. The fluid that wets the medium is referred as the wetting phase, while the other fluid is referred non-wetting phase. For oil-water system, water is mostly the wetting phase and oil the non-wetting phase.

Two-phase flow model is no much different from the single phase, however new concepts are introduced. These include *saturation*, *capillary pressure* and *relative permeability*

3.6.1 Saturation (S)

Phase saturation is the fraction of the pore space of the porous medium that is occupied/filled by that phase. For a two-phase system the sum of the saturation of both the wetting and non-wetting phases is unity: (Knut-Andreas and Bradley, 2016)

$$s_w + s_o = 1 \quad (3.32)$$

where subscript w, o indicates the water and oil phase respectively.

3.6.2 Capillary Pressure (P_c)

As a result of surface tension together with the curvature of the interface between the two phases inside the small pores, the pressure of the non-wetting phase is greater than that of the wetting phase. This results in a pressure difference between the pressures of the fluids concerned given by

$$p_c = p_o - p_w \quad (3.33)$$

3.6.3 Relative Permeability ($K_{r\alpha}$)

Relative permeability is the ratio of the effective permeability k_α , for flow of each of the two fluids to the permeability K of the medium at a given saturation. In a case where a phase does not transition to another, as one phase displaces the other, the phase saturations change. In the displacement process, the ability for movement of one phase is affected by its interaction with the other phase. In macroscopic models, this effect is referred to as the relative permeability. This is dimensionless and a scaling factor depending on saturation and it modifies the absolute permeability to count for reduced ability of the rock to transport each phase in the presence of other phases (Knut-Andreas and Bradley, 2016). It is defined as

$$k_{r\alpha} = \frac{k_\alpha}{K} \quad \alpha \in \{o, w\} \quad (3.34)$$

where $k_{r\alpha}$ is the relative permeability for phase α , k_α is the effective permeability of phase α and K is the absolute permeability.

Except for the term accounting for the mass of the fluid, the derivation of equation (3.25) also apply in deriving flow equations for each of the phase. In the two-phase, the quantity of mass for each phase in a differential volume is the product of the porosity, the density of the phase and the saturation of the phase. Hence we extend

equation (3.25), to obtain the continuity equation for two-phase flow as:

$$\frac{\partial}{\partial t} (\phi \rho_\alpha S_\alpha) + \nabla \cdot (\rho_\alpha \vec{v}_\alpha) = q_\alpha, \quad \alpha \in \{o, w\} \quad (3.35)$$

with

$$\vec{v}_\alpha = -\frac{K k_{r\alpha}}{\mu_\alpha} \nabla (p_\alpha + \rho_\alpha g h) \quad \alpha \in \{o, w\} \quad (3.36)$$

By combining equation (3.32), (3.33), (3.35) and (3.36), the system of differential equations that describe the two-phase (oil-water) flow is obtained as

$$\frac{\partial}{\partial t} (\phi \rho_o S_o) + \nabla \cdot (\rho_o \vec{v}_o) = q_o \quad (3.37a)$$

$$\frac{\partial}{\partial t} (\phi \rho_w S_w) + \nabla \cdot (\rho_w \vec{v}_w) = q_w \quad (3.37b)$$

$$s_w + s_o = 1 \quad (3.37c)$$

$$p_o - p_w = p_c \quad (3.37d)$$

where

$$\vec{v}_o = -\frac{K k_{ro}}{\mu_o} \nabla p_o \quad (3.38a)$$

$$\vec{v}_w = -\frac{K k_{rw}}{\mu_w} \nabla p_w \quad (3.38b)$$

with the assumption that flow is horizontal and as such there is no gravity effect. Another significant factor in modeling two-phase flow is the phase mobility, which is the ability of one phase to move with respect to the movement of the other phase. It is usually denoted as λ_α , $\alpha \in \{o, w\}$ with the expression

$$\lambda_\alpha = \frac{k_{r\alpha}}{\mu_\alpha} \quad (3.39)$$

3.7 Fractional Flow Formulation

According to Yufei et al. (2007), difficulties arise when equation (3.37) with (3.38) is to be solved simultaneously for the four unknown variables (S_α and p_α , $\alpha \in$

$\{o, w\}$). The simultaneous solution results in a strongly or fully coupled system. And according to Yufei et al. (2007), when the implicit scheme is used for the fully coupled system, long computing time is taken for the simulation process, and it becomes much difficult if small element sizes and time steps are used for accuracy.

In this study, fractional formulation identical to the fully coupled system is considered, in order to control the difficulties in simulating fully coupled system. This formulation can be traced back in the petroleum engineering literature, and uses the saturation of one of the two phases and a global/total pressure as the dependent variables. The fractional flow formulation considers the multi-phase flow problem as a total fluid flow of a single mixed fluid, and describes each phase as a fraction of the total fluid flow. This approach results into two equations which is the global pressure equation and the saturation equation for one phase (Tore and Eyvind, 2008). This new system of equations from the fractional flow approach is equivalent to the fully coupled system.

3.7.1 Pressure Differential Equation

Compressible Fluid Flow

Naturally equation (3.37a-b) is reformulated to obtain a flow equation for pressure and transport equation for saturation (Knut-Andreas and Bradley). This is done by expanding the time derivatives in equation (3.37). This results in:

$$\rho_w S_w \frac{\partial}{\partial t} \phi + \phi S_w \frac{\partial}{\partial t} \rho_w + \rho_w \phi \frac{\partial}{\partial t} S_w + \nabla \cdot (\rho_w \vec{v}_w) = q_w \quad (3.40a)$$

$$\rho_o S_o \frac{\partial}{\partial t} \phi + \phi S_o \frac{\partial}{\partial t} \rho_o + \rho_o \phi \frac{\partial}{\partial t} S_o + \nabla \cdot (\rho_o \vec{v}_o) = q_o \quad (3.40b)$$

Dividing through equation (3.40a) by ρ_w and equation (3.40b) by ρ_o , putting the two resulting equations together and using equation (3.37c), equation (3.41) is obtained

$$\frac{\partial}{\partial t} \phi + \phi S_w \frac{1}{\rho_w} \frac{\partial}{\partial t} \rho_w + \phi S_o \frac{1}{\rho_o} \frac{\partial}{\partial t} \rho_o + \frac{1}{\rho_w} \nabla \cdot (\rho_w \vec{v}_w) + \frac{1}{\rho_o} \nabla \cdot (\rho_o \vec{v}_o) = Q_t \quad (3.41)$$

where $Q_t = \frac{q_w}{\rho_w} + \frac{q_o}{\rho_o}$

Fluid and rock compressibility property is defined as:

$$c_r = \frac{1}{\phi} \frac{\partial \phi}{\partial p} \quad c_w = \frac{1}{\rho_w} \frac{\partial \rho_w}{\partial p} \quad c_o = \frac{1}{\rho_o} \frac{\partial \rho_o}{\partial p} \quad (3.42)$$

Using the definition in (3.42) and $c_\alpha \nabla p_\alpha = \frac{1}{\rho_\alpha} \nabla \rho_\alpha$, $\alpha \in \{o, w\}$ we obtain

$$\phi c_r \frac{\partial p}{\partial t} + \phi S_w c_w \frac{\partial p_w}{\partial t} + \phi S_o c_o \frac{\partial p_o}{\partial t} + \vec{v}_w c_w \nabla p_w + \nabla \vec{v}_w + \vec{v}_o c_o \nabla p_o + \nabla \vec{v}_o = Q_t \quad (3.43)$$

Substituting equation (3.38) we obtain

$$\begin{aligned} \phi c_r \frac{\partial p}{\partial t} + \phi S_w c_w \frac{\partial p_w}{\partial t} + \phi S_o c_o \frac{\partial p_o}{\partial t} - c_w \nabla p_w K \lambda_w \nabla p_w - \nabla \cdot (K \lambda_w \nabla p_w) \\ - c_o \nabla(p_o) K \lambda_o \nabla(p_o) - \nabla \cdot (K \lambda_o \nabla(p_o)) = Q_t \end{aligned} \quad (3.44)$$

Simplifying (3.44), the pressure differential equation for a compressible fluid flow is obtained as

$$\begin{aligned} c_w \left(\phi S_w \frac{\partial p_w}{\partial t} - \nabla p_w k \lambda_w \nabla p_w \right) + c_o \left(\phi S_o \frac{\partial p_o}{\partial t} - \nabla(p_o) K \lambda_o \nabla(p_o) \right) \\ + \phi c_r \frac{\partial p}{\partial t} - \nabla \cdot (K \lambda_w \nabla p_w) - \nabla \cdot (K \lambda_o \nabla(p_o)) = Q_t \end{aligned} \quad (3.45)$$

where λ_α is the phase mobility of α , c_r the rock compressibility c_w the wetting phase (water) compressibility, c_o the non-wetting phase (oil) compressibility and Q_t is a specific volumetric injection/production rate term (Luna and Hildago, 2015).

Incompressible Fluid flow

In the particular case of an incompressible fluid flow ($c_r = c_o = c_w = 0$), equation (3.45) becomes

$$-\nabla \cdot (K \lambda_w \nabla p_w) - \nabla \cdot (K \lambda_o \nabla(p_o)) = Q_t \quad (3.46)$$

Expressing the total velocity \vec{v} as a function of the global pressure (p) given by

(Luna and Hildago (2015))

$$\vec{v} = -K(\lambda_w + \lambda_o)\nabla \cdot p \quad (3.47)$$

and letting $\lambda = \lambda_o + \lambda_w$, the pressure differential equation for an incompressible fluid flow is given by

$$-\nabla \cdot (K\lambda\nabla p) = Q_t \quad (3.48)$$

where λ is the total mobility.

3.7.2 Saturation Equation

In this study, the formulation of the saturation equation is done in terms of the wetting phase saturation S_w . With the assumption that the two phases (oil and water) are immiscible is very essential for the fractional formulation. When two immiscible fluids are in contact, there exists between the two fluids a clearly defined interface.

3.7.3 Fractional Flow Function

The fractional flow function is used in calculating the fraction of flow of the total water flow, at any point in the reservoir, with the assumption of a known water saturation at that point. To arrive at the fractional flow formulation for the transport equation for saturation, a fractional flow function (the ratio of mobility of a phase to the total mobility) is define as:

$$f_\alpha(S) = \frac{\lambda_\alpha}{\lambda} \quad \alpha \in \{o, w\} \quad (3.49)$$

where

$$\lambda = \lambda_w + \lambda_o \quad (3.50)$$

The phase mobilities λ_α $\alpha \in \{o, w\}$ are functions of water saturation hence f_α . Fractional flow function is key in multi-phase flow models, since it describes the

fraction of flow of the total water flow at any point in the reservoir. A graph of the fractional flow curve against water saturation is shown in Figure 3.5.

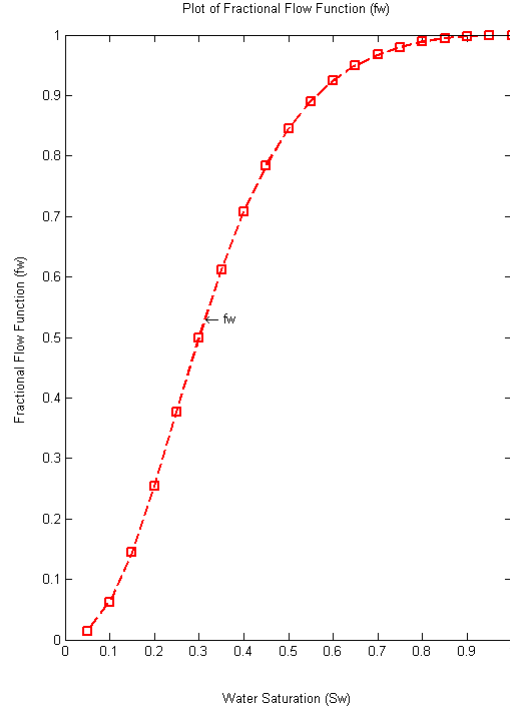


Figure 3.5: The fractional flow curve as a function of Water Saturation

Let \vec{v} be the total velocity defined as

$$\vec{v} = \vec{v}_w + \vec{v}_o \quad (3.51)$$

In the case of an incompressible fluid flow, we can write from the mass balance equation (3.37a-b):

$$\phi \frac{\partial}{\partial t} S_o + \nabla \cdot \vec{v}_o = \frac{q_o}{\rho_o} \quad (3.52a)$$

$$\phi \frac{\partial}{\partial t} S_w + \nabla \cdot \vec{v}_w = \frac{q_w}{\rho_w} \quad (3.52b)$$

Formulating the saturation equation in terms of the wetting phase (water), we use the water saturation equation

$$\phi \frac{\partial}{\partial t} S_w - \nabla \cdot (K \lambda_w \nabla p_w) = \frac{q_w}{\rho_w} \quad (3.53)$$

From equation (3.51), we have

$$\vec{v} = -K\lambda_o\nabla p_o - K\lambda_w\nabla p_w \quad (3.54)$$

Substituting for $p_o = p_c + p_w$ and solving for ∇p_w , we get

$$\nabla p_w = \frac{-\vec{v} - K\lambda_o\nabla p_c}{K(\lambda_w + \lambda_o)} \quad (3.55)$$

Now substituting equation (3.55) into (3.53) and using the fractional flow function in equation (3.49) and simplifying we obtain a convective-diffusive equation:

$$\phi \frac{\partial}{\partial t} S_w + \nabla \cdot (f_w \vec{v}) + \nabla \cdot (K\lambda_o f_w \nabla p_c) = \frac{q_w}{\rho_w} \quad (3.56)$$

where $\nabla \cdot (f_w \vec{v})$ is the convective term and $\nabla \cdot (K\lambda_o f_w \nabla p_c)$, the diffusive term. However in the case where capillary pressure is assumed zero, we obtain a hyperbolic differential equation for saturation.

3.7.4 Residual Saturation

As the reservoir is drained, wetting phase saturation decreases and capillary pressure increases. Finally, a wetting phase saturation is reached, at which point the saturation does not decrease again. The corresponding wetting phase saturation (usually greater than zero) is called *wetting phase residual saturation* S_{wr} . At this point it is not possible to reduce the wetting phase saturation below residual saturation by pure displacement, however, it can be reduced by phase transition, in this case vaporization. As the residual saturation is approached a large increase in capillary pressure produces practically no decrease in wetting phase saturation. It is this large derivative of the capillary pressure function that will require special care in the numerical solution. According to Bastian (1999), the effective water saturation, \bar{S}_w with the residual saturations can be defined as:

$$\bar{S}_w = \frac{S_w - S_{wr}}{1 - S_{wr} - S_{or}} \quad (3.57)$$

The residual saturation in the case of a heterogeneous porous media may depend on position.

3.7.5 Relative Permeability Functions

Relative permeability is defined as a function of phase saturation. $K_{r\alpha}$ for the two-phase case has been defined known as Van Genuchten and Brooks-Correy functions.

Van Genuchten Relative Permeability:

The Van Genuchten relative permeability functions for a two-phase system are written in terms of the residual saturation as

$$k_{rw} = \bar{S}_w^{1/2} \left(1 - \left(1 - \bar{S}_w^{\frac{n}{n-1}} \right)^{\frac{n-1}{n}} \right)^2 \quad (3.58)$$

$$k_{ro} = \bar{S}_o^{1/3} \left(1 - \left(1 - \bar{S}_o \right)^{\frac{n}{n-1}} \right)^{\frac{2(n-1)}{n}} \quad (3.59)$$

where $n \in \{2, 3, 4, 5\}$

Brooks-Correy Relative Permeability:

The Brooks-Correy model is an extension of the work done by Burdine (1953). Burdine developed a functional relationship among effective permeability, saturation and capillary pressure. From this relations, Correy in 1954 proposed the relative permeability model

$$k_{rw}(S_w) = \bar{S}_w^4 \quad (3.60)$$

However in 1964, Correy co-authored with Brooks extended this model to:

$$k_{rw} = \bar{S}_w^{\frac{2+3\gamma}{\gamma}} \quad (3.61)$$

where γ is found to be related to the distribution of the pore size (Brooks and Correy, 1964). Equation (3.61) was derived on the basis that equation (3.60) cannot be valid for all porous media because permeability and saturation are not unique

functions of capillary pressure, but depends upon the size and arrangement of the pores. As a result, a general relation is needed between saturation and capillary pressure that will lead to a wide range of media, leading to equation (3.61). Similarly, relative permeability is defined for the non-wetting phase (oil) as:

$$k_{ro} = \bar{S}_o^2 \left(1 - (1 - \bar{S}_o)^{\frac{2+\gamma}{\gamma}} \right) \quad (3.62)$$

The relative permeability curve for the two phases (wetting and non-wetting) as defined by Brooks and Correy is shown in Figure 3.6

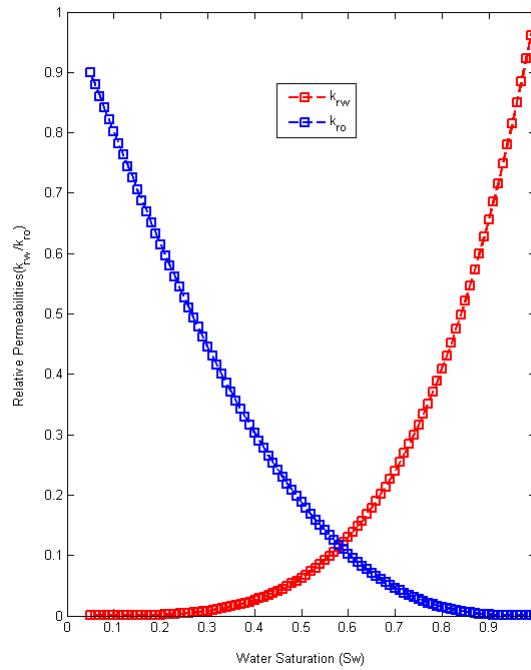


Figure 3.6: Brooks-Correy relative permeability curve for wetting and non-wetting phase

3.7.6 Capillary Pressure Function

The curved interface between the two phases (wetting and the non-wetting) results in a pressure difference between the two phases called the Capillary pressure and is given by

$$p_c(S_w) = p_o - p_w > 0 \quad \text{at the interface}$$

Van Genuchten in 1980, derived capillary pressure function for two phase water-gas system which is written in terms of the effective saturation as:

$$p_c(S_w) = \frac{1}{\alpha} \left(\bar{S}_w^{-\frac{1}{m}} - 1 \right)^{-\frac{1}{n}}, \quad m = 1 - \frac{1}{n}, \quad n \in \{2, 3, 4, 5\} \quad (3.63)$$

where α is in relation to the entry pressure p_d .

Brooks and Correy (1964) defined the capillary pressure function as:

$$p_c(S_w) = p_d \bar{S}_w^{-\frac{1}{\gamma}} \quad 0.2 < \gamma < 3.0 \quad (3.64)$$

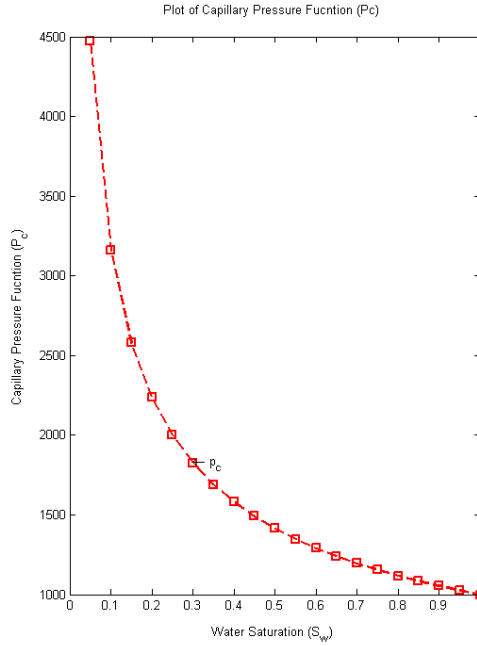


Figure 3.7: A capillary pressure-saturation curve during drainage (Brooks-Correy Capillary pressure function).

Consider the capillary pressure curve, Figure (3.7), at the point $S_w = 1$, with 100% water saturated core sample, the water is gradually displaced by the oil, referred as a *drainage process* with the capillary pressure increasing to a value p_d without a noticeable decrease in S_w . At this water saturation (S_w close to zero) there is an apparent discontinuity at which the saturation of water is not possible to be reduced further, regardless of the imposed difference in phase (capillary) pressure.

The value p_d is called the entry pressure and it is the critical pressure that must be applied for the non-wetting phase to enter the largest pores of the porous medium. If the experiment is reversed, by displacing the oil with water, the process is called the *imbibition process*.

According to Dake (1978), drainage and imbibition processes have a considerable effect on capillary pressure curve for water-oil system where water is the wetting phase. The plot for the two processes are shown in Figure 3.8. The difference in the two plots was observe due to hysteresis in contact angle.

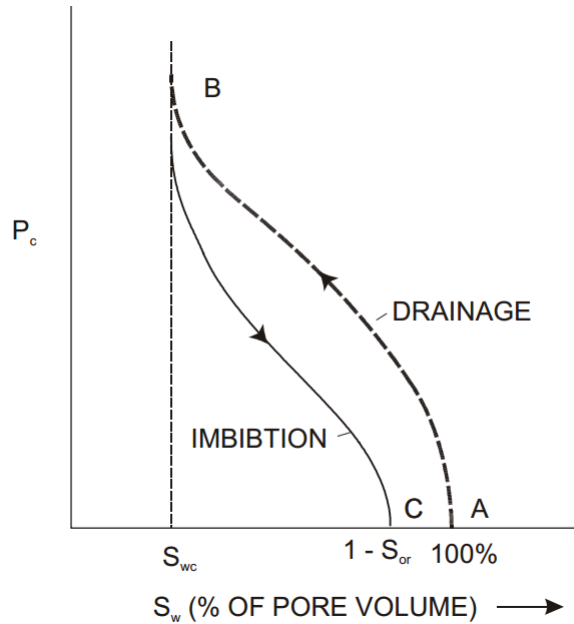


Figure 3.8: Drainage and imbibition capillary pressure functions. Source: L. P. Dakes (1978)

3.8 Model Assumptions

The study of fluid movement in a porous media is more complex. For this reason, certain assumptions are introduced in order to simplify the complexity of models developed (Luna and Hildago, 2015). The following assumptions are established:

- The flow of fluid takes place in one direction (one-dimensional).

- The fluid considered is immiscible with constant composition over time, hence transfer of mass between the phases is not allowed.
- Incompressible fluids are assumed, meaning density is constant over time.
- Since flow is assumed horizontal gravity effect is neglected.

3.9 The Numerical Schemes

Most simulation problems are difficult to be solved analytically, and must instead be solved numerically. Many phenomena in nature are described by partial differential equations involving first and second spatial derivatives and time derivatives of multidimensional functions. Examples of such equations are Maxwell's equations, the heat equation, and the Schrödinger wave equation. Neither differential equations, integral equations, nor integro-differential equations could be solved symbolically or analytically, in general. Nevertheless, we want to simulate these phenomena in order to have insight in these problems. To do so numerical methods are used.

A numerical method for solving a differential equation problem involves discretizing this problem, with infinitely many degrees of freedom, to produce a discrete problem, with finitely many degrees of freedom which is possible to be solved by the use of computers (Zhangxin et al., 2006). Most numerical methods involve an approximation to the unknown function u by a new function u_{ap} which is a linear combination of basis functions

$$u_{ap} = \sum_{i=1}^n u_i \phi_i(x) \quad (3.65)$$

where n is the number of basis functions, u_i are the unknown coefficients, $\phi_i(x)$ are the chosen basis functions, and x is the domain variable, possibly multidimensional (Heckbert, 1993). The finite element and the finite volume methods follow this technique.

3.10 The Variational Method or Weak Formulation

To solve a differential equation by the method of variation, the differential equation is first written in a weighted-integral form, and then an approximate solution for the problem assumed (Reddy, 1993). In approximating numerically an exact solution we are typically replacing an infinite expansion with a finite representation. Such approximation necessarily means that the differential equation cannot be satisfied everywhere in our region of interest and so we are only able to satisfy a finite number of conditions. Since the approximate solution is not likely to equal the exact solution of the differential equation it is likely to have an error in the approximating solution. Consider the linear differential equation (3.66) in the domain Ω :

$$\mathbb{L}(u) = 0 \tag{3.66}$$

where $\mathbb{L}(u)$ is a differential equation having all non-zero terms at the left hand side (for example, $u'' + f = 0$), subjected to suitable initial and boundary conditions. The assumption is that the exact solution, $u_e(x, t)$ can accurately be represented by the approximate solution which is of the form:

$$u_{ap} = u_0(x, t) + \sum_{j \in I_s} u_j(t) \phi_j(x) \quad I_s \in \{0, 1, 2 \dots N\} \tag{3.67}$$

where ϕ_j are analytic functions called *trial* functions and $u_j(t)$ are the N unknown coefficients and $u_0(x, t)$ is chosen to satisfy the initial and boundary conditions. Substitution of the approximate solution (3.67) into equation (3.66) produces a non-zero residual R such that

$$\mathbb{L}(u_{ap}) = R(u_{ap}). \tag{3.68}$$

When approximating a function, the key idea is to minimize the square norm of

the approximate error, $u_e(x, t) - u_{ap}(x, t)$, or to demand that the residual R is orthogonal to a weight or test function $v_i(x)$.

To determine the coefficients $u_j(t)$, equation (3.68) is multiplied by a test function $v_i(x)$ orthogonal to the residual R so that

$$(R(u_{ap}), v_i(x)) = 0 \quad i \in I = \{0, 1, 2, \dots, N\}, \quad (3.69)$$

where the inner product (g, h) of the two functions g and h over the domain Ω is expressed as

$$(g, h) = \int_{\Omega} g(x)h(x)dx \quad (3.70)$$

The weighted residual in the case of (3.69) is said to be zero. The function $v_i(x)$ is the test or weight function defined such that $v = 0$ on the boundaries of the domain. Using integration by parts and an appropriate boundary conditions to equation (3.69) yields the variational or weak form of the differential equation (3.66) which consist of determining the solution $u(x)$ such that

$$a(u, v) = l(v) \quad (3.71)$$

or the problem of looking for the solution $u(x)$ which will minimize the functional

$$I(u) = a(u, v) - l(v) \quad (3.72)$$

where $a(u, v)$ is a bilinear functional of first order derivatives and $l(v)$ is a linear function in terms of the weight or test functions.

Definition 3.10.1 *Let X be a vector space. A mapping $a : X \times X \rightarrow \mathbb{R}$ is called a bilinear form if for arbitrary $\alpha, \beta \in \mathbb{R}$ and $\mathbf{u}, \mathbf{v}, \mathbf{w} \in X$ the following holds:*

$$a(\alpha\mathbf{u} + \beta\mathbf{v}, \mathbf{w}) = \alpha a(\mathbf{u}, \mathbf{w}) + \beta a(\mathbf{v}, \mathbf{w}) \quad (3.73)$$

$$a(\mathbf{u}, \alpha\mathbf{v} + \beta\mathbf{w}) = \alpha a(\mathbf{u}, \mathbf{v}) + \beta a(\mathbf{u}, \mathbf{w}) \quad (3.74)$$

The bilinear form is symmetric if $a(\mathbf{u}, \mathbf{v}) = a(\mathbf{v}, \mathbf{u})$ holds for all $\mathbf{v}, \mathbf{u} \in X$

Definition 3.10.2 Let X be a vector space. A mapping $l : X \rightarrow \mathbb{R}$ is linear if for arbitrary $\alpha, \beta \in \mathbb{R}$ and $\mathbf{v}_1, \mathbf{v}_2 \in X$

$$l(\alpha\mathbf{v}_1 + \beta\mathbf{v}_2) = \alpha l(\mathbf{v}_1) + \beta l(\mathbf{v}_2) \quad (3.75)$$

In looking for an approximate solution to the integrated form of the problem using the approach of Galerkin or Ritz, one looks for a solution in a finite dimensional subspace of the true solution space. By the method of Ritz, an approximate solution that minimizes the functional $I(u)$ is sought to the function. However by the approach of Galerkin, an approximate solution of (3.71) is directly sought for.

According to George and Spencer (1999), the method of weighted residuals illustrates how the choice of different weight (or test) functions in an integral or weak form of the equation can be used to construct many of the common numerical methods. A list of the most commonly used test functions and the computational method they produce is shown in table (3.2).

Table 3.2: Test functions $v_j(x)$ used in the method of weighted residuals and the method produced. Source: (George and Spencer, 1999)

Test Function	Type of Method
$v_i(x) = \delta(x - x_i)$	Collocation
$v_i(x) = \begin{cases} 1 & \text{inside } \Omega^i \\ 0 & \text{outside } \Omega^i \end{cases}$	Finite Volume (Sub-domain)
$v_i(x) = \frac{\partial R}{\partial u_i}$	Least-squares
$v_i(x) = x^i$	Method of Moments
$v_i(x) = \phi_i$	Galerkin
$v_i(x) = \Phi_j (\neq \phi_i)$	Petrov-Galerkin

3.11 The Finite Volume Method

For problems of any finite dimension in continuum, the values of the variables of interest (whether it is temperature, pressure or any other quantity) are infinitely many. This is because these variables are functions of each generic point in the domain or the region of solution. As a result, a continuum problem is one having an infinite number of unknowns. However, since the problem is best solved by reducing it to one of a finite number of unknowns, the finite volume and the finite element discretization techniques are employed. This is achieved by dividing the solution domain into finite volumes or elements.

A more convenient discretization method for the numerical simulation of different types of conservation laws such as parabolic, hyperbolic or elliptic type is the finite volume method. This method has been used considerably in a number of engineering fields including fluid mechanics, mass and heat transfer or in the area of petroleum engineering. The finite volume method comes with some important features which are similar to some characteristics of the finite element method (Idelsohn and Onate, 1993) and (Zienkiewicz and Onate, 1990). The finite volume method may be employed on arbitrary geometries, either by the use of structured meshes or unstructured meshes, leading to robust schemes. In addition using finite volume method makes the numerical fluxes locally conservative (that is the flux is conserved numerically from one discretization cell to its neighbour). The local conservativity of the finite volume makes it somewhat attractive in modeling problems such as in fluid mechanics for which much importance is attached to the flux. Since the finite-volume method is based on a “balanced” approach, it is locally conservative. A local balance is written on control volumes. Using the divergence formula results in an integral formulation of the fluxes on the boundaries of the discretized cell. The boundary fluxes are then discretized in respect of the discrete unknowns.

In one spatial dimension, the finite-volume method basically depends on dividing

the spatial domain into cells or control volumes making in each of them an approximation of the integral of the conservative variables. A constant, $\bar{u}^k(t)$, at the mid-point, x_k , of the control volume defined as $[x_{k-1/2}, x_{k+1/2}]$ approximates the solution of the problem $u(x, t)$. For every time step, the values obtained are updated by approximating the flux at the ends of every interval.

3.12 The Finite Element Method

A numerical technique that can be used in attaining approximate solutions to a number of problems in the field of engineering is the finite element method. This method is a direct implementation of the Galerkin (or Rayleigh-Ritz) procedure with a choice of basis functions (also sometimes called finite element shape functions). After the integral or weak form of the differential equation is formulated, the finite elements starts by discretizing the entire domain Ω into sub-domains called *finite elements* (Courant, 1943). The process of discretizing the domain into finite elements is called *tessellation*. With the increase number of sub domains finite element method gives an accurate approximate solution.

The approach to finite elements throughout the early period has been variational (Pelosi, 2007). Rayleigh-Ritz and Galerkin as example of variational methods have different integral form, weighting functions, and/or approximating functions. Some difficulties associated with Classical method of variation is the construction of its approximating functions for any arbitrary domain (Reddy, 1993). Reddy (1993) discussed the three main features of finite element method giving it superiority over classical method of variation. Firstly, more complex domains can be broken down into a collection of simple sub-domains geometrically (hence the name finite elements). Secondly, approximate functions can be derived with the assumption that continuous functions can be well-approximated as a linear combination of algebraic polynomials over the domain of each finite element . Finally, satisfying the governing equations of each element, the undetermined coefficients are obtained.

The implementation of finite element method starts with the usage of simple interpolation functions as basis functions at the element level after which solution for the entire domain is represented by assembling associated contributions with every element.

3.12.1 The Finite Element Basis Functions

The basis functions are piecewise polynomials of low order with compact support. Denote by $\phi_i(\mathbf{x})$, the finite element basis functions are defined such that they have the property

$$\phi_i(\mathbf{x}_j) = \delta_{ij} = \begin{cases} 1 & i = j \\ 0 & i \neq j \end{cases} \quad (3.76)$$

With this property, then for $u_{ap}(\mathbf{x}) = \sum u_j(t)\phi_j(\mathbf{x})$ we have

$$u_{ap}(\mathbf{x}_i) = \sum u_j(t)\phi_j(\mathbf{x}_i) = \sum u_i(t)\phi_i(\mathbf{x}_i) = u_i(t)$$

which is the value of $u_{ap}(\mathbf{x})$ at node \mathbf{x}_i if the function is independent of time. As a result, the approximate solution $u_{ap}(\mathbf{x}_i)$ will be non-zero for elements with common node \mathbf{x}_j .

3.12.2 One-Dimensional Elements

In a one-dimensional domain $[0, L]$, polynomial elements are defined in terms of a sequence of element endpoints x_i , where $0 = x_0 \leq x_1 \leq x_2 \leq \dots \leq x_n = L$. This sequence of elements is a one-dimensional mesh. Constant elements employ a box basis function that is 1 inside the interval $x_i \leq x \leq x_{i+1}$ and 0 outside (see Figure 3.9(a)), defined as;

$$\text{Box: } \phi_i(x) = \begin{cases} 1 & \text{if } x_i \leq x \leq x_{i+1} \\ 0 & \text{otherwise} \end{cases} \quad (3.77)$$

Linear elements also employ two half hat basis functions, one that rises from 0 to 1 across the interval, and one which falls from 1 to 0 (see Figure 3.9(b)), defined as

$$\text{Hat: } \phi_i(x) = \begin{cases} \frac{x-x_{i-1}}{x_i-x_{i-1}} & \text{if } x_{i-1} \leq x \leq x_i \\ \frac{x_{i+1}-x}{x_{i+1}-x_i} & \text{if } x_i \leq x \leq x_{i+1} \\ 0 & \text{otherwise} \end{cases} \quad (3.78)$$

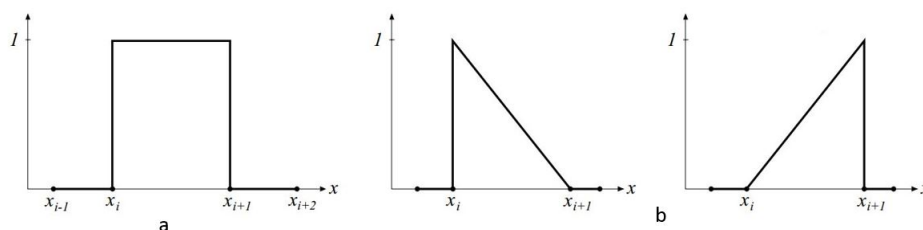


Figure 3.9: (a) Box basis function (b) Left and right half hat basis functions.

Quadratic and higher degree elements are common as well. The choice of basis functions is somewhat arbitrary. The most commonly used basis functions in the finite element literature are defined in terms of Lagrange interpolation. The degrees of freedom are chosen to be the value of the function at selected points. Formulas for these are most easily given in terms of a *master element* with domain $p \in [0, L]$. This master element can be scaled and translated to map it to any interval using the transformation $x = (x_{i+1} - x_i)p - x_i$. To create a degree d element, $d - 1$ points are chosen in the master interval, such that $0 < p_0 < p_1 < \dots < p_d = 1$. Lagrange polynomial of degree d , for $i = 0, 1, \dots, d$ is

$$L_i^d(p) = \prod_{j=0, j \neq i}^d \frac{p - p_j}{p_i - p_j} \quad (3.79)$$

Quadratic Lagrange polynomials are shown in Figure 3.10, and a degree d Lagrange is shown in Figure 3.11.

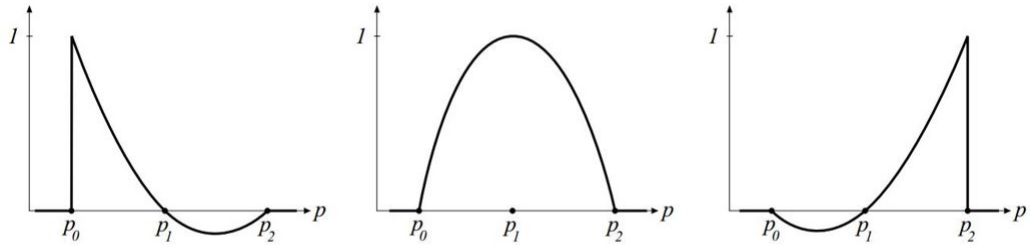


Figure 3.10: Basis functions for quadratic Lagrange interpolation.

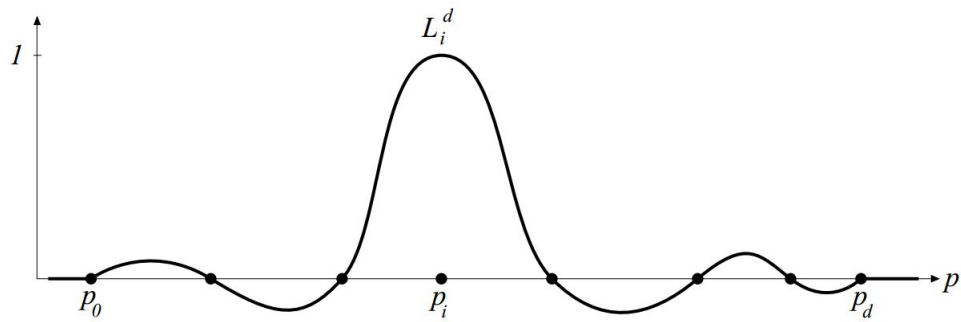


Figure 3.11: Basis functions for degree d Lagrange interpolation at node i .

This basis function has value 1 at $p = p_i$ and value 0 at all other nodes p_j . The box and half hat basis functions given earlier are just the degree 0 and degree 1 Lagrange basis functions respectively.

Chapter 4

NUMERICAL IMPLEMENTATION OF THE TWO-PHASE FLOW MODEL

4.1 Problem Formulation

The two-phase flow problem with the effect of capillary pressure is formulated from equation (3.48) and (3.56) with initial and boundary conditions as:

$$\left\{ \begin{array}{l} \text{Find } p, S_w \in \Omega \rightarrow \mathbb{R} \text{ such that} \\ -\nabla \cdot (K\lambda\nabla p) = Q_t \quad \text{on } \Omega \\ \phi \frac{\partial}{\partial t} S_w + \nabla \cdot (f_w \vec{v}) + \nabla \cdot (K\lambda_o f_w \nabla p_c) = \frac{q_w}{\rho_w} \quad \text{on } \Omega \end{array} \right. \quad (4.1)$$

with initial conditions

$$S_w = \begin{cases} 0.05 & (x = 0) \\ 0 & (0 < x \leq 1km) \end{cases}$$

and boundary condition

$$\left\{ \begin{array}{l} p(0, t) = p(t) \quad \text{on } \Gamma_D \\ -K\lambda \left(\frac{\partial p}{\partial x} \right)_{x=l} = \frac{Q(t)}{A} \quad \text{or} \quad \partial_n (-K\lambda\nabla p) = g_1 = \frac{Q(t)}{A} \quad \text{on } \Gamma_N \end{array} \right.$$

where

$$Q_t = \frac{q_w}{\rho_w} + \frac{q_o}{\rho_o}, \quad \lambda = \lambda_o + \lambda_w, \quad \text{with } \lambda_o = \frac{k_{ro}}{\mu_o} \quad \text{and} \quad \lambda_w = \frac{k_{rw}}{\mu_w},$$

the total velocity given by

$$\vec{v} = -K(\lambda_o + \lambda_w) \frac{\partial}{\partial x} p$$

and the fractional flow function given by

$$f_w = \frac{\lambda_w}{\lambda_o + \lambda_w}.$$

In this work, the Brooks-Corey relative permeability function and capillary pressure function is employed for the numerical simulation of the problem. The relative permeability and capillary pressure functions according to Brooks and Corey are given respectively by Equation (4.2) and (4.3) as:

$$k_{rw} = \bar{S}_w^{\frac{2+3\gamma}{\gamma}}, \quad k_{ro} = \bar{S}_o^2 \left(1 - (1 - \bar{S}_o)^{\frac{2+\gamma}{\gamma}}\right) \quad (4.2)$$

and

$$p_c(Sw) = p_d \bar{S}_w^{-\frac{1}{\lambda}} \quad 0.2 < \lambda < 3.0 \quad (4.3)$$

where \bar{S}_α , $\alpha \in \{o, w\}$ is the effective phase saturation defined in Equation (3.57) with the assumption that the residual saturation is zero, hence $\bar{S}_w = S_w$ and $\bar{S}_o = S_o$.

In the case where there is no capillary pressure effect, the two-phase problem is formulated with initial and boundary conditions as:

$$\left\{ \begin{array}{l} \text{Find } p, S_w \in \Omega \rightarrow \mathbb{R} \text{ such that} \\ -\nabla \cdot (K \lambda \nabla p) = Q_t \quad \text{on } \Omega \\ \phi \frac{\partial}{\partial t} S_w + \nabla \cdot (f_w \vec{v}) = \frac{q_w}{\rho_w} \quad \text{on } \Omega \end{array} \right. \quad (4.4)$$

with initial conditions

$$S_w = \begin{cases} 0.05 & (x = 0) \\ 0 & (0 < x \leq 1km) \end{cases} \quad (4.5)$$

and boundary condition

$$\begin{cases} p(0, t) = p(t) & \text{on } \Gamma_D \\ -K\lambda \left(\frac{\partial p}{\partial x}\right)_{x=l} = \frac{Q(t)}{A} \text{ or } \partial_n(-K\lambda\nabla p) = g_1 = \frac{Q(t)}{A} & \text{on } \Gamma_N \end{cases} \quad (4.6)$$

The problem is solved using Finite Element-Finite Volume method and the numerical approximation for the problem is done in 1-dimensional space hence $\nabla u = \frac{\partial}{\partial x}u$.

4.2 FE-FV Implementation for the Two-Phase Problem With Capillary Pressure Effect

To solve problem (4.1), the elliptic pressure equation is approximated by the Finite element method and the advective-diffusive saturation equation solved using the Finite Volume Method.

4.2.1 Weak Formulation for the Pressure Equation

To solve the pressure equation with the Finite element method, the problem in the strong form is first written in a weak or variational form. To write the problem in the weak form, the Neumann boundary condition and the pressure differential equation are multiplied by a test function v from which equation (4.7) and (4.8) are obtained.

$$\int_{\Omega} [\nabla \cdot (K\lambda\nabla p) + Q_t] v d\Omega = 0 \quad (4.7)$$

$$\int_{\Omega} [\partial_n(K\lambda\nabla p) + g_1] v d\Omega = 0 \quad (4.8)$$

Greens theorem states that

$$\int_{\Omega} \nabla(\nabla u)v + \int_{\Omega} \nabla u \nabla v = \int_{\Gamma} (\partial_n u)v. \quad (4.9)$$

Using the Greens theorem, results in (4.10)

$$\int_{\Gamma} \partial_n(K\lambda\nabla p)v d\Gamma - \int_{\Omega} (K\lambda\nabla p)\nabla v d\Omega + \int_{\Omega} Q_t v d\Omega = 0 \quad (4.10)$$

Define the following spaces

$$\begin{aligned} L^2(\Omega) &= \{f : \Omega \rightarrow \mathbb{R} \mid \int |f|^2 < \infty\} \\ H^1(\Omega) &= \{u \in L^2(\Omega) \mid \nabla u \in L^2(\Omega)\} \\ H_0^1(\Omega) &= \{u \in H^1(\Omega) \mid u = 0 \text{ on } \Gamma_D\}. \end{aligned}$$

Using the Neumann boundary condition, and the fact that the test function must satisfy homogeneous condition on the Dirichlet boundary (i.e. $v = 0$ on Γ_D), equation (4.10) becomes

$$\int_{\Omega} (K\lambda\nabla p)\nabla v d\Omega = \int_{\Omega} Q_t v d\Omega - \int_{\Gamma_N} g_1 v d\Gamma \quad (4.11)$$

Now the weak form of the pressure equation for problem (4.1) is written as

$$\left\{ \begin{array}{l} \text{Find } p \in H^1(\Omega) \text{ such that} \\ p(0, t) = p(t) \quad \text{on } \Gamma_D \\ \int_{\Omega} (K\lambda\nabla p)\nabla v d\Omega = \int_{\Omega} Q_t v d\Omega - \int_{\Gamma_N} g_1 v d\Gamma \quad \forall v \in H_0^1(\Omega). \end{array} \right. \quad (4.12)$$

4.3 Well-posedness of the Problem

Well-posedness means the existence and uniqueness of solution and the continuity of the solution with respect to the data (the initial and boundary conditions and the right hand side of the pde). In the sense of Hadamard, a partial differential equation (pde) is well posed iff

1. There exist a solution
2. The solution to the pde is unique

- Solutions depends on the data (the initial and boundary conditions and the right hand side of the pde)

Existence and uniqueness involves boundary conditions. If the pde has too many boundary conditions, the solution may not exist and if the the boundary conditions are too few, solution may not be unique.

4.3.1 Lax-Milgram Lemma

Lax-Milgram Lemma is a basis and most important tool for proving the existence and uniqueness of solution to elliptic problems.

Theorem 4.3.1 (Lax-Milgram) *Let V be a Hilbert Space, $a : V \times V \rightarrow \mathbb{R}$ a bounded V -elliptic bilinear form and l be a linear form. Assume that*

- a is continuous, i.e., there exists a constant $C > 0$ such that*

$$|a(u, v)| \leq C \|u\|_V \|v\|_V \quad \forall u, v \in V \quad (4.13)$$

- a is V -elliptic, i.e., there exists a constant $C > 0$ such that*

$$a(v, v) \geq C \|v\|_V^2 \quad \forall v \in V \quad (4.14)$$

- The linear form l is continuous, i.e., there exists a constant C such that*

$$l(v) \leq C \|v\|_V \quad \forall v \in V \quad (4.15)$$

Then there exists a unique solution to the problem: Find $u \in V$ such that

$$a(u, v) = l(v) \quad \text{for all } v \in V \quad (4.16)$$

Definition 4.3.1 (Dirichlet-Poincare's Inequality) *If $u : \Omega \rightarrow \mathbb{R}$ and $u \in V = H_0^1(\Omega)$, then*

$$\int_{\Omega} |u|^2 \leq C_{\Omega} \int_{\Omega} |\nabla u|^2 \quad \text{where } C_{\Omega} > 0 \quad (4.17)$$

4.3.2 Verification of the Conditions of Lax-Milgram Lemma

To verify the conditions of Lax-Milgram Lemma, rewrite equation (4.12) in one spatial dimension with homogeneous Dirichlet condition in the form; Find $u \in V$ such that

$$a(u, v) = l(v) \quad \text{and} \quad p - p(t) = u = 0 \quad \text{on} \quad \Gamma_D \quad \text{for all } v \in H_0^1(\Omega) \quad (4.18)$$

where the bilinear form is:

$$a(u, v) = \int_0^L \left(K\lambda \frac{\partial}{\partial x} u \right) \frac{\partial}{\partial x} v dx \quad (4.19)$$

and the linear form $l(v)$, is given by:

$$l(v) = \int_0^L Q_t v dx - \int_{\Gamma_N} \frac{Q(t)}{A} v d\Gamma + \int_0^L K\lambda \frac{\partial}{\partial x} p(t) \frac{\partial}{\partial x} v dx \quad (4.20)$$

1. Continuity and boundedness of a :

From the bilinear form,

$$|a(u, v)| = \left| \int_0^L \left(K\lambda \frac{\partial}{\partial x} u \right) \frac{\partial}{\partial x} v dx \right| \leq \int_0^L \left| \left(K\lambda \frac{\partial}{\partial x} u \right) \frac{\partial}{\partial x} v \right| dx \quad (4.21)$$

By Hölder's Inequality, we have

$$|K\lambda| \int_0^L \left| \left(\frac{\partial}{\partial x} u \right) \frac{\partial}{\partial x} v \right| dx \leq |K\lambda| \left(\int_0^L \left| \frac{\partial}{\partial x} u \right|^2 dx \right)^{1/2} \left(\int_0^L \left| \frac{\partial}{\partial x} v \right|^2 dx \right)^{1/2} \quad (4.22)$$

In particular, if g is in the Hilbert space V , then

$$\|g\|_2 = \left(\int_0^L |g|^2 dx \right)^{1/2} \quad (4.23)$$

This implies that

$$|a(u, v)| \leq |K\lambda| \|u\|_{1,2} \|v\|_{1,2} \quad (4.24)$$

Hence $a(u, v)$ is bounded for $u, v \in V$

2. Positivity:

It is obvious that

$$a(v, v) = \int_0^L K\lambda \frac{\partial}{\partial x} v \frac{\partial}{\partial x} v dx \geq 0 \quad \text{for all } v \in V$$

For $a(v, v)$ strictly positive, it is obvious that

$$a(v, v) = \int_0^L K\lambda \frac{\partial}{\partial x} v \frac{\partial}{\partial x} v dx > 0 \quad \text{iff } 0 \neq v \in V$$

3. V -elliptic (coercive):

Assume that $k\lambda$ is strictly positive, from the bilinear form we have

$$a(v, v) = \int_0^L K\lambda \left| \frac{\partial}{\partial x} v \right|^2 dx = k\lambda \int_0^L \left| \frac{\partial}{\partial x} v \right|^2 dx \quad (4.25)$$

From Dirichlet-Poincaré's inequality, $\int_\Omega |\nabla u|^2 \geq \frac{1}{C_\Omega} \int_\Omega |u|^2$. Hence

$$a(v, v) = K\lambda \int_0^L \left| \frac{\partial}{\partial x} v \right|^2 dx \geq \frac{K\lambda}{C_\Omega} \int_0^L |v|^2 dx = \frac{K\lambda}{C_\Omega} \|v\|_{1,2}^2 \quad (4.26)$$

Hence a is V -elliptic

4. Finally, it is shown that $l(v)$ is continuous:

$$|l(v)| \leq \left| \int_0^L Q_t v dx \right| + \left| \int_{\Gamma_N} \frac{Q(t)}{A} v d\Gamma \right| + \left| \int_0^L K\lambda \frac{\partial}{\partial x} p(t) \frac{\partial}{\partial x} v dx \right| \quad (4.27)$$

$$\leq \int_0^L |Q_t v| dx + \int_{\Gamma_N} \left| \frac{Q(t)}{A} v \right| d\Gamma + \int_0^L \left| K\lambda \frac{\partial}{\partial x} p(t) \frac{\partial}{\partial x} v \right| dx \quad (4.28)$$

$$\leq \|Q_t\|_{L^2} \|v\|_{1,2} + |A|^{-1} \|Q(t)\|_{L^2} \|v\|_{1,2} + K\lambda \|p(t)\|_{L^2} \|v\|_{1,2} \quad (4.29)$$

$$= (\|Q_t\|_{L^2} + |A|^{-1} \|Q(t)\|_{L^2} + K\lambda \|p(t)\|_{L^2}) \|v\|_{1,2} \quad (4.30)$$

Hence

$$|l(v)| \leq (\|Q_t\|_{L^2} + |A|^{-1} \|Q(t)\|_{L^2} + K\lambda \|p(t)\|_{L^2}) \|v\|_{1,2} \quad (4.31)$$

Consequently, the solution to the weak form (4.12) is unique and bounded in $H_0^1(\Omega)$

4.3.3 Finite Element Implementation for Pressure Equation

The finite element formulation continues after the weak form (equation 4.12) of the problem is obtained by first discretizing the domain, Ω , into sub-domains, Ω_i (finite elements). Let the entire domain Ω be discretized into sub-domains Ω_i (finite elements). Define a space of functions V_h given by

$$V_h = \{u_h \in L^2(\Omega) | \nabla u_h \in L^2(\Omega)\}$$

and $V_h^{\Gamma_D} \subset V_h$ given by

$$V_h^{\Gamma_D} = \{u \in V_h | u = 0 \text{ on } \Gamma_D\}$$

This results in the discrete problem

$$\left\{ \begin{array}{l} \text{Find } p_h \in V_h \text{ such that} \\ p_h(0, t) = p(t) \quad \text{on } \Gamma_D \\ \int_{\Omega} (K\lambda \nabla p_h) \nabla v_h d\Omega = \int_{\Omega} Q_t v_h d\Omega - \int_{\Gamma_N} g_1 v_h d\Gamma \quad \forall v_h \in V_h^{\Gamma_D} \end{array} \right. \quad (4.32)$$

From the solution space V_h , let $v_h = \phi_j(x) \in V_h^{\Gamma_D}$ be finite element basis function defined on the nodes for each element. Again let the approximate solution be the linear combination

$$p_h(x, t) = p(t) + \sum_{i=1}^N \phi_i(x) p_i(t)$$

where $p_i(t)$ are the nodal values of pressure varying with time and $\phi_i(x)$ the nodal

basis functions. The term $p(t)$ is to account for the Dirichlet boundary condition. Substituting v_h , $p_h(x, t)$ and g_1 into (4.32) and simplifying results in the linear system of equation

$$\sum_{i=1}^N \left(\int_{\Omega} K \lambda \nabla \phi_i(x) \nabla \phi_j(x) \right) p_i(t) d\Omega = \int_{\Omega} Q_t \phi_j(x) d\Omega - \int_{\Gamma_N} \frac{Q(t)}{A} \phi_j(x) d\Gamma \quad (4.33)$$

which can be written in a more compact way as

$$K \lambda M_{ij} p_{w_i}(t) = b_j \quad j = 1, 2, \dots, N \quad (4.34)$$

where

$$M_{ij} = \sum_{i=1}^N \int_{\Omega} \nabla \phi_i(x) \nabla \phi_j(x) d\Omega \text{ and } b_j = \int_{\Omega} Q_t \phi_j(x) d\Omega - \int_{\Gamma_N} \frac{Q(t)}{A} \phi_j(x) d\Gamma$$

4.3.4 FVM for the Saturation Equation with Capillary Pressure Effect

The Saturation profile with the effect of capillary pressure is formulated as

$$\phi \frac{\partial}{\partial t} S_w + \frac{\partial}{\partial x} (f_w \vec{v}) + \frac{\partial}{\partial x} \left(K \lambda_o f_w \frac{\partial}{\partial x} p_c \right) = \frac{q_w}{\rho_w} \quad \text{on } \Omega \quad (4.35)$$

with initial conditions

$$S_w = \begin{cases} 0.05 & (x = 0) \\ 0 & (0 < x \leq 1km) \end{cases}$$

In proving for the existence and uniqueness of the saturation equation, an energy estimate for the saturation is derived (see (Schroll and Tveito, 2000)). Schroll and Tveito (2000) in their study, proved for the local existence and uniqueness for the saturation equation. Consequently, the existence and uniqueness of the saturation equation with the capillary pressure.

To solve the saturation equation by Finite volume method, the domain is discretized

into several sub-cells $S_i = \{x_{i-1/2}, x_{i+1/2}\}$ called control volume and write

$$\int_{x_{i-1/2}}^{x_{i+1/2}} \phi \frac{\partial}{\partial t} S_w dx + \int_{x_{i-1/2}}^{x_{i+1/2}} \frac{\partial}{\partial x} (f_w \vec{v}) dx + \int_{x_{i-1/2}}^{x_{i+1/2}} \frac{\partial}{\partial x} \left(K \lambda_o f_w \frac{\partial}{\partial x} p_c \right) dx = \int_{x_{i-1/2}}^{x_{i+1/2}} \frac{q_w}{\rho_w} dx \quad (4.36)$$

Let Δx be the cell length. Dividing through by Δx gives

$$\begin{aligned} & \phi \frac{1}{\Delta x} \int_{x_{i-1/2}}^{x_{i+1/2}} \frac{\partial}{\partial t} S_w dx + \frac{1}{\Delta x} \int_{x_{i-1/2}}^{x_{i+1/2}} \frac{\partial}{\partial x} (f_w \vec{v}) dx + \\ & \frac{1}{\Delta x} \int_{x_{i-1/2}}^{x_{i+1/2}} \frac{\partial}{\partial x} \left(K \lambda_o f_w \frac{\partial}{\partial x} p_c \right) dx = \frac{1}{\Delta x} \int_{x_{i-1/2}}^{x_{i+1/2}} \frac{q_w}{\rho_w} dx \end{aligned} \quad (4.37)$$

This is rewritten as

$$\begin{aligned} & \phi \frac{d}{dt} \int_{x_{i-1/2}}^{x_{i+1/2}} \frac{1}{\Delta x} S_w dx + \frac{1}{\Delta x} \left(f_w(S_{w_{i+1/2}}) v_{i+1/2} - f_w(S_{w_{i-1/2}}) v_{i-1/2} \right) + \\ & \frac{1}{\Delta x} \left[\left(K \lambda_o f_w \frac{\partial}{\partial x} p_c \right)_{x_{i+1/2}} - \left(K \lambda_o f_w \frac{\partial}{\partial x} p_c \right)_{x_{i-1/2}} \right] = \frac{q_w}{\rho_w}. \end{aligned} \quad (4.38)$$

Writing $\frac{\partial}{\partial x} p_c \Big|_{x_{i-1/2}} = \frac{p_{c_i} - p_{c_{i-1}}}{\Delta x}$ and $\frac{\partial}{\partial x} p_c \Big|_{x_{i+1/2}} = \frac{p_{c_{i+1}} - p_{c_i}}{\Delta x}$ results in

$$\begin{aligned} & \phi \frac{d}{dt} \int_{x_{i-1/2}}^{x_{i+1/2}} \frac{1}{\Delta x} S_w dx + \frac{1}{\Delta x} \left(f_w(S_{w_{i+1/2}}) v_{i+1/2} - f_w(S_{w_{i-1/2}}) v_{i-1/2} \right) + \\ & \frac{1}{\Delta x} \left[K \lambda_o f_w(S_{w_{i+1/2}}) \frac{p_c(S_{w_{i+1}}) - p_c(S_{w_i})}{\Delta x} - K \lambda_o f_w(S_{w_{i-1/2}}) \frac{p_c(S_{w_i}) - p_c(S_{w_{i-1}})}{\Delta x} \right] = \frac{q_w}{\rho_w} \end{aligned} \quad (4.39)$$

Let $S_{w_i} = \int_{x_{i-1/2}}^{x_{i+1/2}} \frac{1}{\Delta x} S_w dx$ be the cell average. This represents the value of S_w at node i . Using forward difference for the time derivative of S_w , gives

$$\begin{aligned} & \phi \frac{S_{w_i}^{n+1} - S_{w_i}^n}{\Delta t} + \frac{1}{\Delta x} \left(f_w(S_{w_{i+1/2}}) v_{i+1/2} - f_w(S_{w_{i-1/2}}) v_{i-1/2} \right) + \\ & \frac{1}{\Delta x} \left[K \lambda_o f_w(S_{w_{i+1/2}}) \frac{p_c(S_{w_{i+1}}) - p_c(S_{w_i})}{\Delta x} - K \lambda_o f_w(S_{w_{i-1/2}}) \frac{p_c(S_{w_i}) - p_c(S_{w_{i-1}})}{\Delta x} \right] = \frac{q_w}{\rho_w} \end{aligned} \quad (4.40)$$

Consequently, making $S_{w_i}^{n+1}$ the subject, the finite volume implementation for the

saturation equation with the effect of capillary pressure is obtained as

$$S_{w_i}^{n+1} = S_{w_i}^n - \frac{\Delta t}{\phi \Delta x} \left(f_w(S_{w_{i+1/2}})v_{i+1/2} - f_w(S_{w_{i-1/2}})v_{i-1/2} \right) - \frac{\Delta t}{\phi \Delta x} \left[K \lambda_o f_w(S_{w_{i+1/2}}) \frac{p_c(S_{w_{i+1}}) - p_c(S_{w_i})}{\Delta x} - K \lambda_o f_w(S_{w_{i-1/2}}) \frac{p_c(S_{w_i}) - p_c(S_{w_{i-1}})}{\Delta x} \right] + \frac{\Delta t}{\phi} \frac{q_w}{\rho_w}. \quad (4.41)$$

However, in the case where the capillary pressure is considered negligible, modeled by equation (4.4), the corresponding finite volume implementation for the saturation equation is obtained as

$$S_{w_i}^{n+1} = S_{w_i}^n - \frac{\Delta t}{\phi \Delta x} \left(f_w(S_{w_{i+1/2}})v_{i+1/2} - f_w(S_{w_{i-1/2}})v_{i-1/2} \right) + \frac{\Delta t}{\phi} \frac{q_w}{\rho_w}. \quad (4.42)$$

Upwind Scheme

The upwind scheme is used for advection dominated problems. It allows us to find the saturation values at the grid points instead of the interface. Since $S_{w_{i-1/2}}$ are the interface values of the saturation, they need to be expressed in terms of the cell averages (evaluated at the grid points) by using the upwind scheme. As a result, $S_{w_{i+1/2}}$ and $S_{w_{i-1/2}}$ are then expressed in terms of the cell averages by the upwind schemes respectively as:

$$S_{w_{i+1/2}}^n = \begin{cases} S_{w_i} & \text{if } v(x_i, t^n) > 0 \\ S_{w_{i+1}} & \text{if } v(x_i, t^n) < 0 \end{cases} \quad (4.43)$$

and

$$S_{w_{i-1/2}}^n = \begin{cases} S_{w_{i-1}} & \text{if } v(x_i, t^n) > 0 \\ S_{w_i} & \text{if } v(x_i, t^n) < 0 \end{cases} \quad (4.44)$$

4.3.5 Courant-Friedrichs-Lewy (CFL) Condition

Since the saturation scheme for both cases (i.e., Saturation equation with and without Capillary effect) in the finite volume approach is explicit, its stability is impor-

tant. Hence the Courant-Friedrichs-Lewy (CFL) condition must be applied. CFL is a necessary condition for convergence while solving partial differential equations by the method of finite difference. It arises in the numerical analysis of explicit time integration scheme. The CFL condition has the form:

$$C = \frac{\Delta t}{\Delta x} \leq C_{\max} \quad (4.45)$$

For explicit schemes, Δt and Δx are chosen such that $C_{\max} = 1$. However for implicit schemes larger values of C_{\max} may be tolerated since implicit schemes are less sensitive to numerical instability.

4.3.6 Approach to Solving the Coupling Pressure-Saturation Equation

The pressure and saturation equations are solved following a similar strategy employed by Luna and Hildago (2015)

- Step 1: The pressure equation is solved using the FEM, beginning with initial water saturation profile: $s_w(x, 0)$, considering the intervals $[x_i, x_{i+1}]$ as finite elements. The nodal values for the pressure, p_i , are calculated.
- Step 2: From the Darcy's law (Equation 3.38b), the velocity values are computed at each node x_i from p_i . The pressure gradients are evaluated by the use of a reconstruction procedure by Luna and Hildago (2015). The slope for the pressure was chosen according to: $|m_i| = \min(|m_{i,-1}|, |m_{i,1}|)$ where $m_{i,-1} = \frac{p_i - p_{i-1}}{\Delta x}$ and $m_{i,1} = \frac{p_{i+1} - p_i}{\Delta x}$
- Step 3: The interface fluxes are computed from the nodal values of the velocity by introducing the interface velocities in $f_w(S_{i+1})v_{i+1}$.
- Step 4: These fluxes are then substituted into the saturation equation to solve for the saturation using the initial saturation profile to evaluate the capillary terms.

Chapter 5

NUMERICAL RESULTS, DISCUSSION AND CONCLUSION

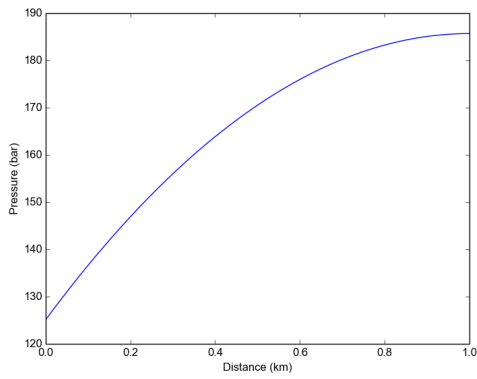
5.1 Numerical Results and Discussion

The numerical results obtained in this work for the problem without the capillary effect (equation 4.4) are shown in Figure 5.1-???. These results illustrate the pressure and saturation profile for the two-phase flow model without the capillary pressure effect.

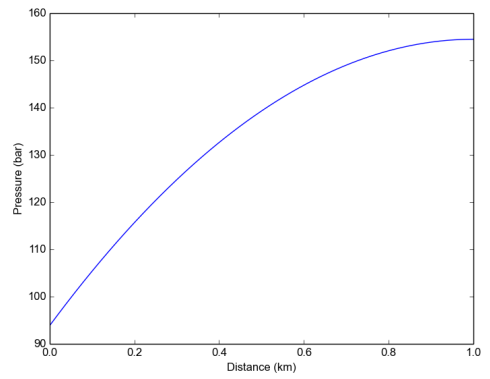
Naturally fluids flow from a region of high pressure to a region of low pressure. From the results, it is observed that the reservoir pressure evolves at initial time $t = 0$, from an initial value of about 185.646 bar at the end of the reservoir ($x = 1$) to 125 bar at ($x = 0$) (satisfies the boundary condition at $x = 0$ at time zero). With a higher pressure 185.646 bar applied at the end $x = 1$ of the reservoir, it is observed that the pressure declines from the end of the reservoir ($x = 1$) to the well-bore ($x = 0$) hence flow of fluid is towards the well-bore as expected. Finally, it is also observed that the pressure profile decreases with time. This is evident in Figure 5.2.

In imbibition process, where oil is being displaced (i.e., oil production) by water, it is expected that, oil saturation should be decreasing with time for increasing water saturation. And since the reservoir is completely filled by the fluid in place, it is expected that the oil and water saturation sum to one at any particular time.

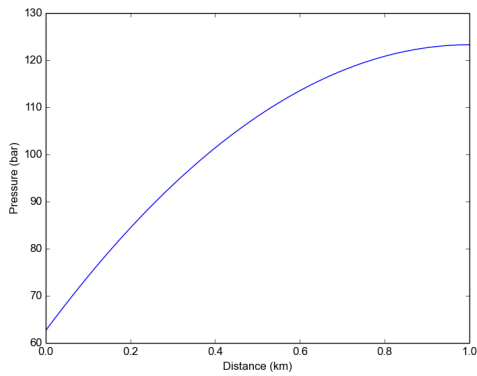
From the numerical results obtained from the saturation profiles of both oil and



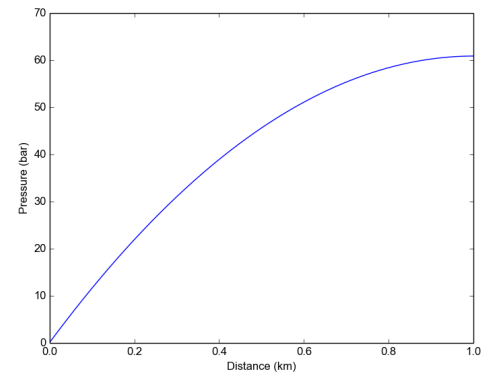
(a) Pressure Profile at $t=0$



(b) Pressure Profile at $t=0.25$



(c) Pressure Profile at $t=0.50$



(d) Pressure profile at $t=1.0$

Figure 5.1: Plot showing the Pressure profile, (p) along the distance for different time values

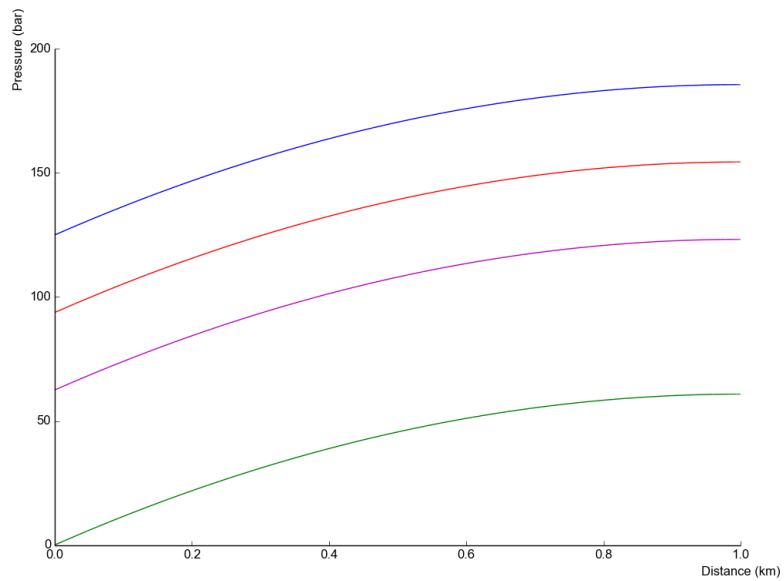


Figure 5.2: Pressure profile at $t=0$ (Blue), $t=0.25$ (Red), $t=0.5$ (Magenta), $t=1$ (Green)

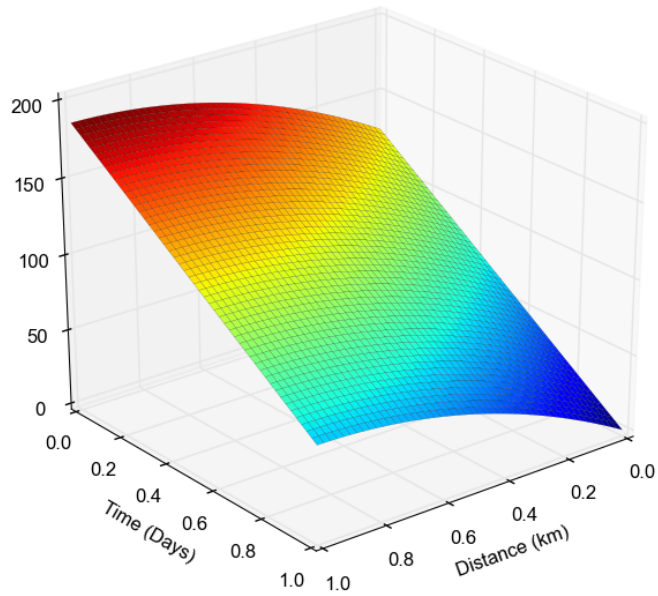


Figure 5.3: Surface plot of Pressure profile (p)

water as shown in Figure ?? and 5.4, it can be observed that the two profiles exhibits the expected behavior for imbibition process. Comparing both profiles from Figure 5.4, at a particular time t , it is evident that the sum of the saturation values for oil and water is 1, and also as the water saturation increases from t_0 to t_1 , the oil saturation decreases correspondingly.

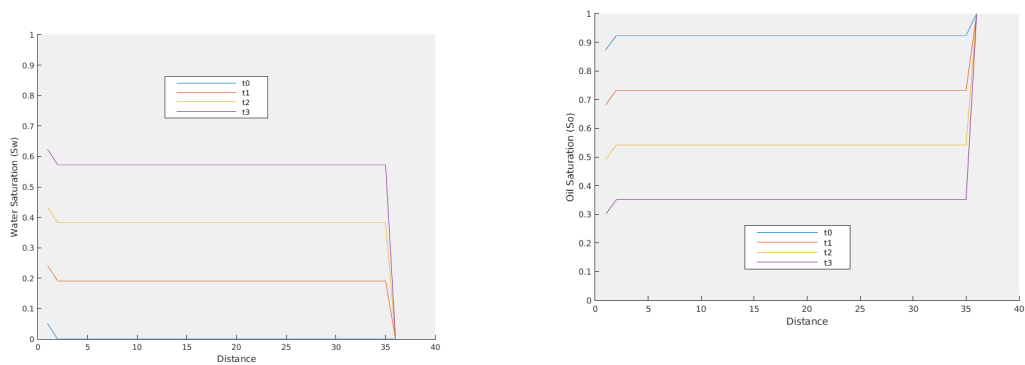


Figure 5.4: Plot showing the saturation profile (S_w, S_o) of water and oil along the distance for different time values

5.2 Investigating the Effect of Capillary Pressure

5.2.1 Capillary Pressure Effect on Flow Rate

According to Dake (1978), the fractional flow equation (without gravity effect) for the displacement of oil by water, in one dimension is given by:

$$f_w = \frac{1 + \frac{k k_{ro} A}{q_t \mu_o} \frac{\partial p_c}{\partial x}}{1 + \frac{\mu_w}{k_{rw}} \cdot \frac{k_{ro}}{\mu_o}} \quad (5.1)$$

The effect of the capillary pressure gradient term $\frac{\partial p_c}{\partial x}$, could be understood qualitatively by rewriting the gradient term as

$$\frac{\partial p_c}{\partial x} = \frac{\partial p_c}{\partial S_w} \cdot \frac{\partial S_w}{\partial x} \quad (5.2)$$

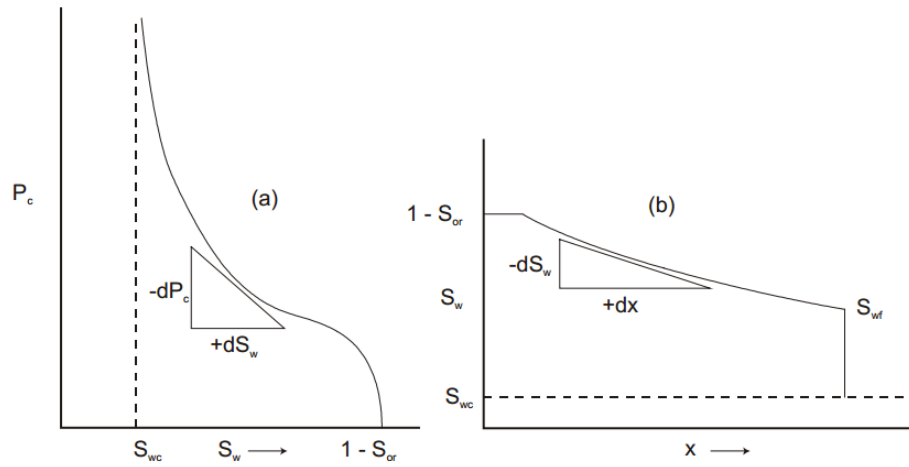


Figure 5.5: (a) Capillary pressure function ; (b) water saturation distribution as a function of distance in the displacement path. (Source: L. P. Dakes, 1978)

From Figure 5.5(a), the slope of the capillary pressure curve, $\frac{\partial p_c}{\partial S_w}$, is negative as well as the slope of the water saturation profile in respect to flow direction . Therefore $\frac{\partial p_c}{\partial x}$ will be positive at all time, hence the capillary pressure gradient term present increases the fractional flow of water.

5.2.2 Capillary Pressure Effect on Saturation Profile

Fluid flow in a reservoir can be advective, diffusive or both advective and diffusive in nature. Advection is the motion of particles along the bulk flow. Diffusion is the net movement of particles from high concentration to low concentration. In order to investigate the effect of capillary pressure on fluid flow, numerical simulation of the two-phase flow model with the capillary pressure effect was investigated considering two different cases. Under the two situations, the reservoir model was run under the same reservoir conditions.

Case 1 (Diffusion Dominated Flows): In order to demonstrate the capillary pressure effect on saturation in diffusive dominated flows, we set $v = 0$ in the transport equation (4.1b) of the model problem. In our model, flow of fluid by diffusion is accounted for by the diffusive term which has the capillary pressure function, (p_c) . The results indicate that, capillary pressure is the main drive of fluids in diffusion processes which is made evident in (Figure5.6a).

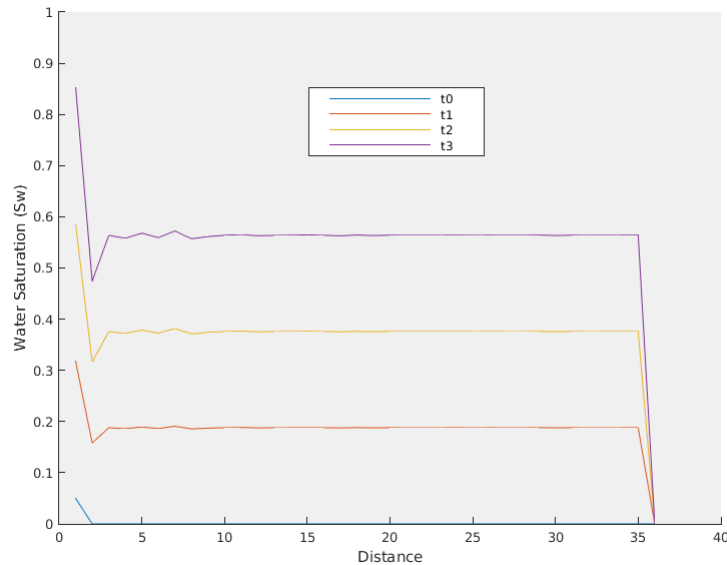
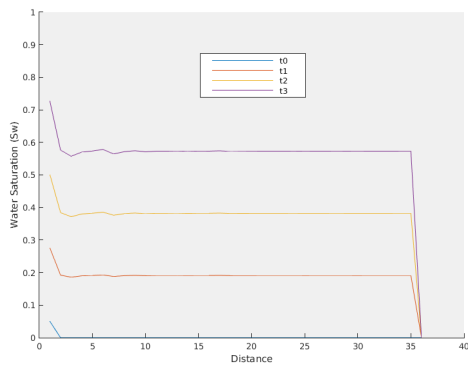


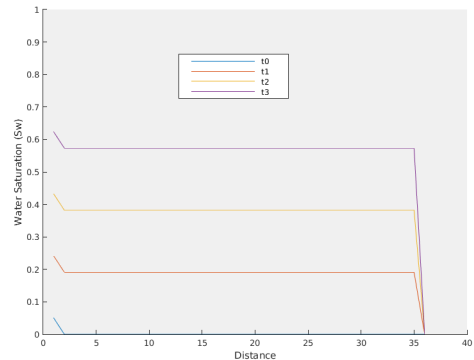
Figure 5.6: Fluid flow by diffusion ($p_c \neq 0$)

Case 2 (Flow by advection and diffusion): Secondly, to investigate the capillary pressure effect on fluid transport in advective flows, the transport equation

was solved numerically with the diffusive term. The numerical simulation for the advection-diffusion equation (4.1b) was run and the result compared to the saturation profile without the diffusive term (capillary pressure) under the same reservoir conditions.



(a) Fluid flow by advection and diffusion ($p_c \neq 0$)



(b) Fluid flow by advection ($p_c = 0$)

Figure 5.7: Comparison of Saturation (S_w) profile for fluid flow by advection/diffusion with advection

It is observed that, the distribution for the saturation profiles in these two situations (i.e., advection-diffusion and advection only) are notably different near the well-bore - which is as a result of the presence of the capillary pressure term - but has similar behavior as one moves further away from the well-bore.

5.3 Conclusions

In this work, we have demonstrated the effect of capillary pressure on the two-phase flow model. The two-phase fluid flow model with the effect of capillary pressure was successfully modeled resulting into a non-linear system of partial differential equations which was reformulated to obtain an elliptic partial differential equation for pressure, a parabolic or convective-diffusive equation for saturation using the fractional flow formulation. This new formulation enabled effective simulation of the flow model under capillary pressure conditions by allowing us to employ two different methods - finite element and the finite volume methods - for the descri-

zation of the pressure and the saturation equation.

The capillary pressure effect on the saturation profile was further studied in this work by considering two cases - diffusion dominated case and advection-diffusion case. From the findings it was observed that in situations where flow of fluid in a reservoir is dominated by diffusion, the advance of fluid is mainly by the effect of capillary pressure. Finally, in a situation where flow is by both advection and diffusion, the capillary pressure is to be considered for dynamic processes where saturation gradient is large. However for dynamic processes where there is little or no saturation change, the capillary pressure can be considered negligible or zero.

According to literature, porosity ϕ , and permeability K , which were assumed constant in this study, are discontinuous functions in real cases, which in effect could have some level of influence on fluid transport. Hence for further studies, the effect of these reservoir properties, porosity and permeability, can be investigated to explore their effect on fluid dynamics in a porous medium.

5.4 Recommendation

Reservoir properties such as porosity ϕ , and permeability K , may as well have some influences on fluid transport in a porous medium. According to literature, porosity and permeability which were assumed constant in this study, are discontinuous functions in real cases, which in effect could have some level of influence on fluid transport. Hence for further studies, the effect of these reservoir properties, porosity ϕ and permeability K , can be investigated to explore their effect on fluid dynamics in a porous medium.

REFERENCES

- Aarnes, J., Kippe, V., Knut-Andreas, L., and Rustad, A. B. (2007). Modeling of multiscale structures in flow simulations for petroleum reservoirs. *Geometric Modelling Numerical Simulation and Optimization*. Accessed online: July, 2016.
- Bastian, P. (1999). *Numerical Computation of Multiphase Flows in Porous Media*. PhD thesis, Christian-Albrechts, Heidelberg.
- Bear, J. and Bachmat, J. (1991). *Introduction to Modeling of Transport Phenomena in Porous Media*. Kluwer Academic Publisher.
- Bergamaschi, L., Mantica, S., and Manzini, G. (1998). A mixed finite element-finite volume formulation of the black-oil model. *Society for Industrial and Applied Mathematics, SIAM J. SCI. COMPUT.*, 20:970–997.
- Berndt, M., Lipnikov, K., Shashkov, M., Wheeler, M., and Yotov, I. (2005). Superconvergence of the velocity in mimetic finite difference methods on quadrilaterals. *SIAM J. Numer. Anal.*, 43:7281–749.
- Botero, S., Hassanizadehi, S. M., Kleingeldi, P. J., and Bezuijen, A. (2016). Experimental study of dynamic capillary pressure effect in two-phase flow in porous media. Accessed online: <http://proceedings.dtu.dk/fedora/repository/dtu:1817/OBJ/article.pdf>, July, 2016.
- Brooks, R. and Correy, A. (1964). Hydraulic properties of porous media. *Colorado State University Hydrology Paper*. Colorado State University, 3.
- Burdine, N. T. (1953). Relative permeability calculations from pore-size distribution data. *Trans. AIME*, 198:71–7871.
- Chen, Z. and Zhang, Y. (2009). Well flow models for various numerical methods. *International Journal of Numerical Analysis and Modeling, Institute for Scientific Computing and Information*, 6:375–388.

- Courant, R. L. (1943). Variational methods for the solution of problems of equilibrium and vibration. *Bulletin of the American*, 4,9:1–23.
- Craft, B. C. and Hawkins, M. F. (1991). *Applied Petroleum Reservoir Engineering*. Prentice Hall PTR, Prentice-Hall, Inc., 2nd edition.
- Dake, L. P. (1978). Fundamentals of reservoir engineering. *Elsevier Science B. V., Netherlands*.
- Darcy, H. (1856). Les fontaines publiques de la ville de dijon, paris. *Librairie des Corps Impàriaux des Ponts et Chaussées et des Mines*.
- Eymard, R., Gallouët, T., and Herbin, R. (2016). Finite volume approximation of elliptic problems and convergence of an approximate gradient. *Accessed online: <https://www.cmi.univ-mrs.fr/herbin/PUBLI/convgrad98.pdf>, September, 2016*.
- George, E. K. and Spencer, J. S. (1999). *Spectral/hp Element Methods for CFD*. Numerical Mathematics and Scientific Computation, Oxford University Press.
- Heckbert, P. S. (1993). *Introduction to Finite Element Methods*. Carnegie Mellon University, Global Illumination Course SIGGRAPH.
- Helmer, A. F. and Steinar, E. (2011). Numerical treatment of two phase flow in capillary heterogeneous porous media by finite-volume approximations. *AMS Subject Classifications: 65M60, 76S05, 35R05*.
- Hirsch, C. (1988). *Numerical Computation of Internal and External FLOws*. A Wiley Interscience Publication, John Wiley & Sons, New York.
- Huang, J. and Xi., S. (1998). On the finite volume element method for general self-adjoint elliptic problem. *SIAM J.Numer. Anal.*, 35(5):1762–1774.
- Idelsohn, S. R. and Onate, E. (1993). Finite volumes and finite elements: two good friends. *International Journal for Numerical Methods in Engineering*, 37(19):3323–3341.

- Johnson, C., Nävert, U., and Pitkäranta, J. (1984). Finite element methods for linear hyperbolic problems. *Computer Methods in Applied Mechanics and Engineering, Elsevier Science Publishers B.V. North-Holland*, 45:285–312.
- Klausen, R. and Winther, R. (2014). *Convergence of multipoint flux approximations on quadrilateral grids. Numerical Methods for Partial Differential Equations*,. John Wiley & Sons, Inc.
- Knut-Andreas, L. and Bradley, T. M. (2016). Mathematical models for oil reservoir simulation. Retrieved online: <http://folk.uio.no/kalie/papers/eacm-ressim.pdf>, 20 June, 2016.
- Lazarov, R. D. and Mishev, I. D. (1996). Finite volume methods for reaction-diffusion problems. *Texas A&M University, College Station, TX, U.S.A.*
- Lee, J. K. and Froehlich, D. C. (1986). Review of literature on the finite-element solution of the equations of two-dimensional surface-water flow in the horizontal plane. *U.S. Geological Survey circular*, 1009.
- Luna, P. and Hildago, A. (2015). Mathematical modeling and numerical simulation of two-phase flow problems at pore scale. *Electronic Journal of Differential Equations, Conference 22*, pages 79–97.
- Michael, L. and Ben, S. (2008). Two-phase flow equations with outflow boundary conditions in the hydrophobic-hydrophilic case. *Fakultät für Mathematik, TU Dortmund*, 87:44227.
- Mishev, I. D. and Qian-Yong, C. (2016). A mixed finite volume method for elliptic problems. *ExxonMobil Upstream Research Company*. Accessed online: August 2016.
- Nordbotten, J. M. and Celia, M. A. (2012). Geological storage of co₂: Modeling approaches for large-scale simulation. *A John Wiley & Sons*.
- Paul, G. (2016). Fluid saturation and capillary pressure. *Petrophysics MSc Course Notes*. Retrieved online:

- http://homepages.see.leeds.ac.uk/~earpwjg/PG_EN/CD%20Contents/GGL-66565%20Petrophysics%20English/Chapter%204.PDF, June 2016.
- Pelosi, G. (2007). The finite-element method, part 1: R. l. courant. *IEEE Antennas and Propagation Magazine*, 49.
- Price, H. S., Cavendish, J. C., and Varga, R. S. (1968). Numerical methods of higher-order accuracy for convection-diffusion equations. *Society of Petroleum Engineers Journal*, 8(2):293–303.
- Reddy, J. N. (1993). *Finite element method*. John Wiley and Sons Inc, New York.
- Salarieh, M., Doroudi, A., Sobhi, G. A., and Bashiri, G. (2016). The role of capillary pressure curves in reservoir simulation studies. *Research Inistitute of petroleum Industry*. Accessed Online: <http://www.pogc.ir/Portals/0/maghalat/890720-1.pdf>, July 2016.
- Schroll, H. J. and Tveito, A. (2000). Local existence and stability for a hyperbolic-elliptic system modeling two-phase reservoir flow. *Electronic Journal of Differential Equations*, pages 1–28.
- Shams, M. S., El-Banbi, A. H., and Khairy, M. (2015). Capillary pressure considerations in numerical reservoir simulation studies-conclusion maps. *Society of Petroleum Engineers*.
- Shashkov, M. (1996). *Conservative Finite-difference methods on general grids*. CRC Press, New York.
- Thacker, W. (1978). Comparison of finite-element and finite difference schemes. part 1: One-dimensional gravity wave motion. *Journal of Physical Oceanography*, 8(4):676–679.
- Tore, I. B. and Eyvind, A. (2008). Comparing equations for two-phase fluid flow in porous media. *Excerpt from the Proceedings of the COMSOL Conference, Hannover*.

- Wojciech, S. and Anna, T. (2014). Darcy's and forchheimer's laws in practice. part 1. the experiment. *Technical Sciences*, 17(4):321–335.
- Yufei, C., Birgitte, E., and Rainer, H. (2007). Fractional flow formulation for two-phase flow in porous media. *International Research Training Group GRK 1398/1 "Non-linearities and upscaling in porous media"*.
- Zhangxin, C., Guanren, H., and Yuanle, M. (2006). Computational methods for multiphase flows in porous media. *Society for Industrial and Applied Mathematics*, pages 9–34.
- Zienkiewicz, O. C. and Onate, E. (1990). Finite volumes vs. finite elements. is there really a choice? *CIMNE, Barcelona*,.